General Disclaimer

One or more of the Following Statements may affect this Document

- This document has been reproduced from the best copy furnished by the organizational source. It is being released in the interest of making available as much information as possible.

- This document may contain data, which exceeds the sheet parameters. It was furnished in this condition by the organizational source and is the best copy available.

- This document may contain tone-on-tone or color graphs, charts and/or pictures, which have been reproduced in black and white.

- This document is paginated as submitted by the original source.

- Portions of this document are not fully legible due to the historical nature of some of the material. However, it is the best reproduction available from the original submission.

JPL Contract 951709

STERILIZABLE LIQUID PROPULSION SYSTEM

FINAL REPORT (PART II)

Author

Samuel C. Lukens

This work was performed for the Jet Propulsion Laboratory, California Institute of Technology, as sponsored by the National Aeronautics and Space Administration under Contract NAS7-100.

September 1969

MARTIN MARIETTA CORPORATION
DENVER DIVISION

NOTICE

This report was prepared as an account of Government-sponsored work. Neither the United States, nor the National Aeronautics and Space Administration (NASA), nor any person acting on behalf of NASA:

a. Makes warranty or representation, expressed or implied, with respect to the accuracy, completeness, or usefulness of the information contained in this report, or that the use of any information, apparatus, method, or process disclosed in this report may not infringe privately-owned rights; or

b. Assumes any liabilities with respect to the use of, or for damages resulting from the use of any information, apparatus, method, or process disclosed in this report.

As used above, "person acting on behalf of NASA" includes any employee or contractor of NASA, or employee of such contractor, to the extent that such employees or contractor of NASA, or employee of such contractor prepares, disseminates, or provides access to, any information pursuant to his employment with such contractor.

Requests for copies of this report should be referred to:

National Aeronautics and Space Administration
Office of Scientific and Technical Information
Washington 25, D. C.

Attention: AFSS-A

PT. I - T-4414116

MCR-68-119

STERILIZABLE LIQUID PROPULSION SYSTEM
FINAL REPORT
PART II

September 1969

Author

S C Lukens

Samuel C. Lukens
Program Manager

JPL Contract 951709

This work was performed for the Jet Propulsion Laboratory, California Institute of Technology, as sponsored by the National Aeronautics and Space Administration under Contract NAS7-100.

MARTIN MARIETTA CORPORATION
P. O. Box 179
Denver, Colorado

FOREWORD

This report is submitted in accordance with paragraph (a)(1)(v)(F) of Article 1 and paragraph (b)(6) of Article 2 of Modification No.1 to JPL Contract 951709. This is Part II of two parts.

CONTENTS

I. INTRODUCTION

This is the second and final part of the program final report submitted in accordance with JPL Contract 951709. This Part II covers the period from April 1, 1968 through the completion of the technical effort on May 9, 1969.

The program involved the design, fabrication, and exposure of a fueled bipropellant liquid propulsion system to the ethylene oxide (ETO) and heat sterilization requirements specified by JPL specification VOL-50503-ETS. After exposure the system was then fired for 280 sec.

The program was continued to gather additional information resulting from a second series of sterilization exposure cycles and additional materials compatibility tests. Insofar as possible the propulsion system was reassembled to the initial configuration following evaluation of the effects of the initial exposure and test firing. It was then exposed to three-30-hr.dry heat sterilization cycles and refired for an additional 280 sec.

The initial portion of the program included a materials testing activity and a components test activity wherein early test results could be factored into the design and assembly of the complete propulsion module. The initial portion of the program was completed in March of 1968. Part I of the final report was published as quickly as possible so systems designers might have the benefit of the program results in a timely fashion. The author, in preparing Part II, assumes the reader is familiar with Part I of the report.

The JPL Technical Monitor for the contract was Mr. Merle E. Guenther. The Program Manager for Martin Marietta was Mr. Samuel C. Lukens.

The following personnel at Martin Marietta were major contributors to the follow-on effort:

H. F. Brady, Technical Lead;

C. Holt, Materials Test;

J. B. Keough, Systems Test.

Figure I-1 is a photo of the assembled module in a display stand.

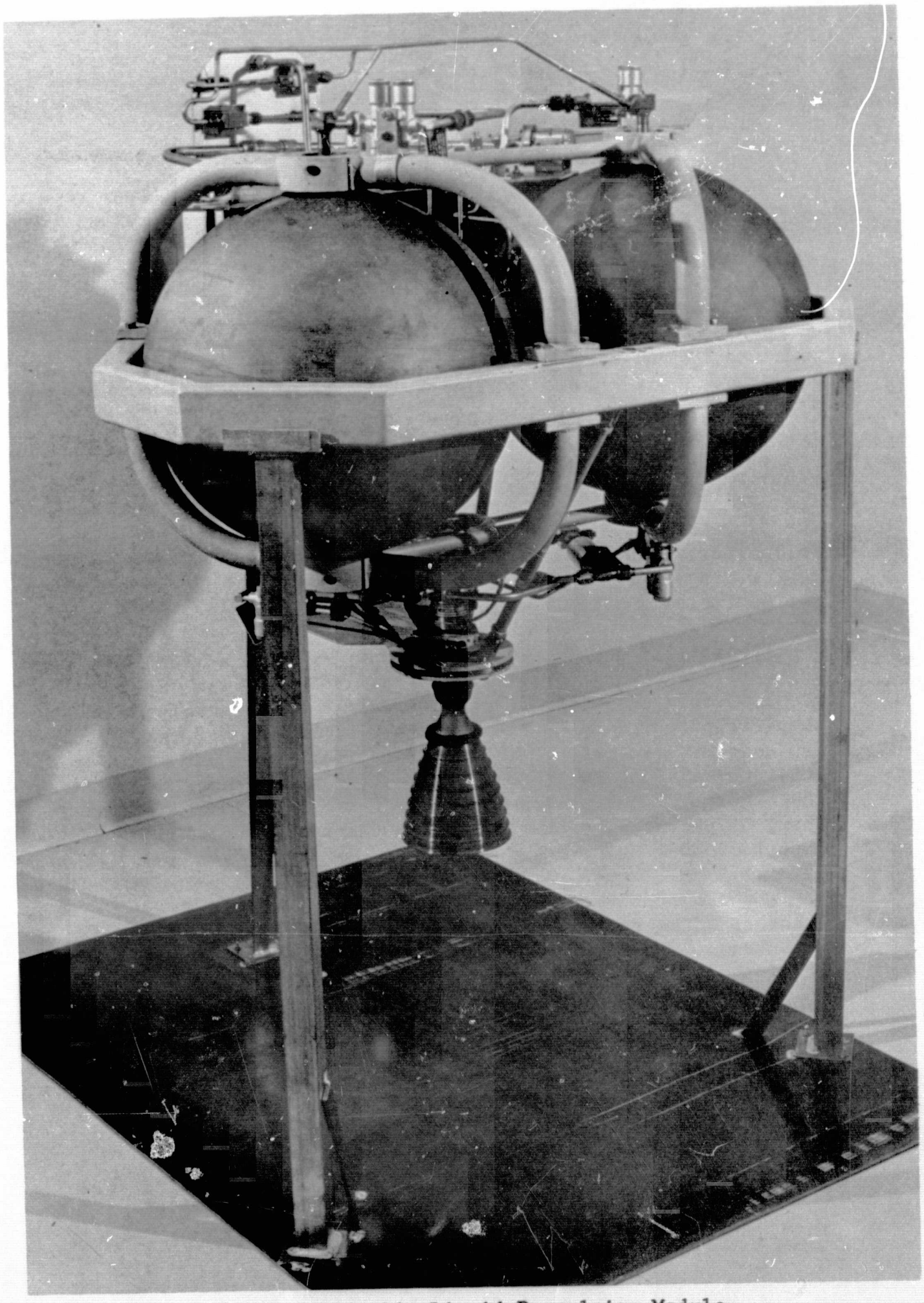

Fig. I-1 Sterilizable Liquid Propulsion Module.

II. PROGRAM PLAN AND OBJECTIVES

A modification to the original contract statement of work directed that the module with corrected components be reassembled, exposed to added dry heat sterilization, and refired for 280 sec. The program objective was to give increased assurance that the propulsion module system would perform satisfactorily through a second demonstration firing.

To implement the above activity several support activities were initiated. A materials compatibility test program was implemented to gather as much additional data as feasible. Twenty-five additional materials specimens were exposed to N_2O_4 at 135°C for 600 hr. The results of the original effort yielded sufficient materials compatibility data in MMH to give the designer an adequate catalog of materials for selection.

A design change was implemented in both the fuel and oxidizer tanks. It was an objective of the program to redesign the fuel tank as necessary to demonstrate -1 g fuel outflow. This was done by making several minor changes in the trap design. Further, the oxidizer tank was redesigned to mount the diaphragm at the centerline so that a symmetrical configuration of the diaphragm would be achieved so that line-to-line contact with the tank wall would be made in either the loaded or expelled position.

With the new tank designs the module was reassembled, loaded with propellant, sterilized for three 30-hr. cycles at 135°C and then test fired. This was a continuation of Task IV of the original program.

Management of the program was implemented by a project organization shown in Fig.II-1. This is the same organization used in the initial program. It is characterized by the direct design and engineering organization shown at the first level supported by manufacturing, quality, and safety shown on the second level. The equipment selection committee was inactive in this portion of the program since no new components were identified or procured.

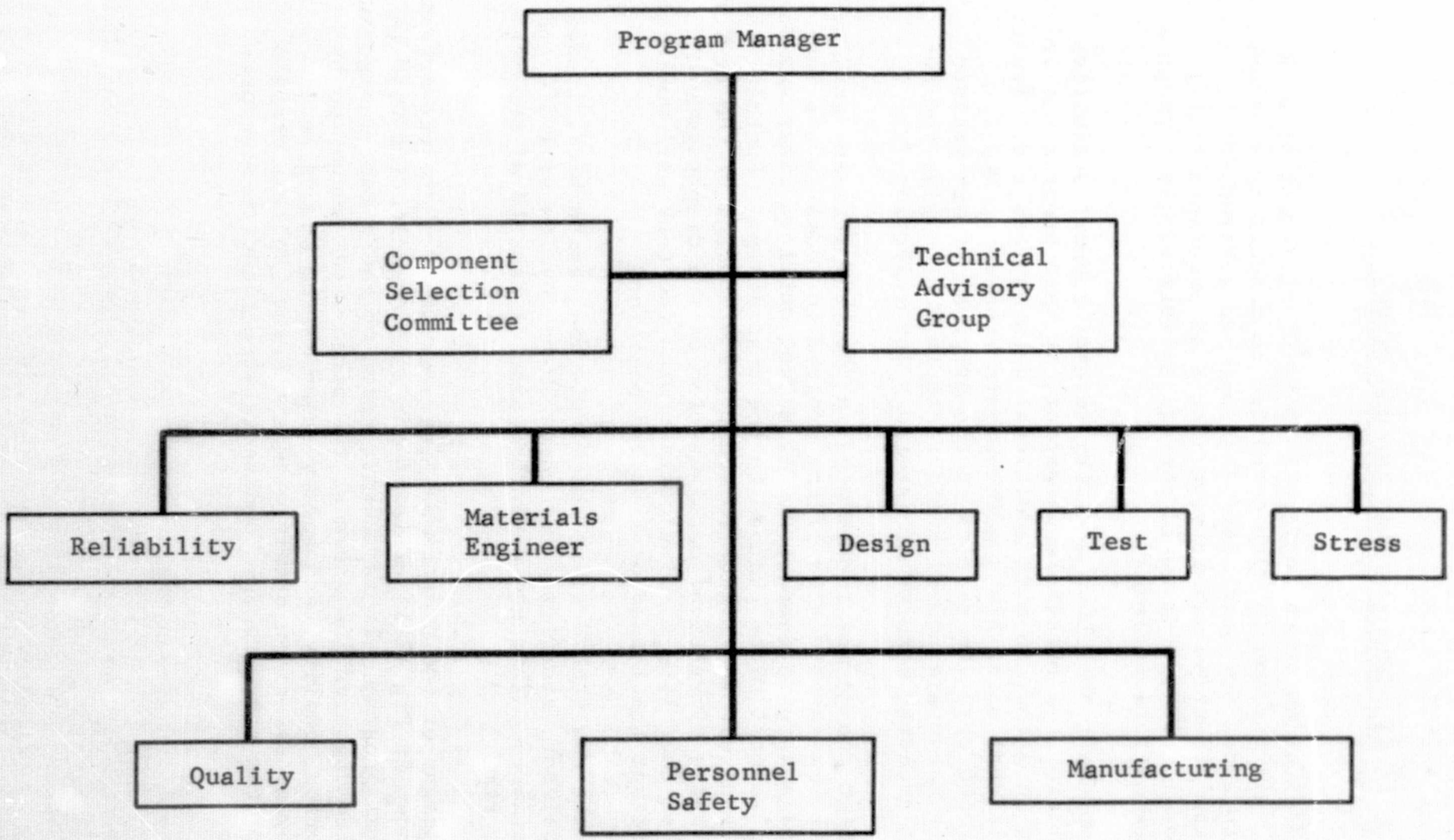

Fig. II-1 Program Organization

III. CONCLUSIONS

The conclusions that can be drawn from the results of this program are itemized below:

1) The cause of the aborted firing attempt was the improper assembly of an ordnance valve. This allowed burning combustion products and melted aluminum to enter the system tubing, which led to a tube failure at a bend in the tube;

2) The remaining system components and the Marquardt engine operated satisfactorily following the second sterilization exposure;

3) The regulator was stuck in the open position after storage of 15 months following the initial system firing demonstration. This malfunction would have seriously jeopardized a planetary mission. The cause was attributed to a coagulated lubricating film in the area of the spring guide and cap assembly. This problem can be solved with no new technology;

4) The hand valves incorporated in the system showed the same degradation as reported in Part I of this report;

5) The design of the oxidizer tank diaphragm girth seal has been adequately demonstrated. Teflon permeation remains an important factor in the diaphragm and tank design;

6) Fabrication and inspection techniques can lead to design problems. The problem is manifested by membrane stretch of the Teflon diaphragm due to inflation for inspection that results in a stress near the yield point;

7) Failure of one of the diaphragms was attributed to maintaining pressure loads after the diaphragm was stretched in a heated condition. Removal of the heat caused the membrane to exceed the ultimate strength, which led to the failure;

8) The trap device installed in the fuel tank successfully provides single phase liquid outflow in a negative 1 g regime;

9) Nickel is a major cause of the corrosion of the 300 series stainless steels;

10) Anodic coatings of aluminum alloys insure a very high degree of protection of these materials;

11) Tantalum, columbium, tungsten, and the ceramics were unaffected by the N_2O_4 exposure at 135°C;

12) Liquid propulsion systems may be qualified for planetary program usage without extending the state of the art.

IV. RECOMMENDATIONS

As a result of the work performed during this portion of the program the following recommendations can be made:

1) Future designs of Teflon diaphragms, bladders, and other similar devices should provide for a line-to-line wall contact with less than 1 percent inflation;

2) Further development should be carried out to determine the proper inspection criteria for the heating and sealing of Teflon coated parts.

3) Aluminum seats, seals, and mechanical parts usage in a propulsion system using N_2O_4 is not recommended. High-strength materials such as titanium should be incorporated using a bellows-type stem seal;

4) The properties of Teflon in the presence of heated nitrogen tetroxide should be more definitive;

5) Tantalum screens should be developed to provide capillary devices for nitrogen tetroxide service in sterilizable systems;

6) In conjunction with recommendation 5), welding development programs should be initiated to provide the capability to weld dissimilar materials without forming incompatible products;

7) The regulator failure mode should be eliminated by knurling the contact surfaces or providing contact lands to reduce the surface area to prevent the sticking. Additional tests should be performed to verify the corrective action;

8) Because of the penalties associated with sterilization of nitrogen tetroxide systems it is recommended a program qualifying a sterile propellant transfer system be initiated at once. This should include bio-assay monitoring to assure program adequacy.

V. TECHNICAL DISCUSSION

A. MATERIALS COMPATIBILITY EVALUATION

1. Background

A continued materials test program produced a number of interesting and valuable results that will serve to broaden the technology developed in the first series of tests conducted in the fourth quarter of 1966 and reported in the second Quarterly Report, April 1967, and Part I of the final report, August 1968. Earlier tests produced sufficient materials data to allow design and functional operation of a sterilizable engine module loaded with propellants before heat sterilization. Materials tested in 1966 exhibited varying degrees of resistance to N_2O_4 at 135°C after 600 hr. A brief summary of those results are listed below:

1) Titanium alloy 6Aℓ-4V possessed the highest degree of resistance to the propellant. This alloy was used for the propellant tanks;

2) All structural aluminum alloys tested were found to sustain both surface and intergranular attack (up to 4 mils deep) with production of finely divided aluminum nitrate salts;

3) The 300 series stainless steels were attacked both at the surface and at grain boundaries to a depth of about 0.004 in. This attack caused the formation of massive quantities of a thick viscous amorphous product that contained the same elements as the parent material;

4) All high nickel alloys were attacked destructively and produced large quantities of semiliquid corrosion products;

5) Teflon was lightly attacked with the production of a white flock with no significant change in the physical properties of the material.

The additional materials compatibility test specimens were selected to evaluate a variety of basic alloys not considered previously and to determine whether protective coatings could be used on materials subject to attack. Other considerations included evaluation of ductile metals for screen devices and the importance of nickel, as an alloying agent, on the corrosion resistance of ferrous-based alloys.

Anodizing is a commonly used practice for providing a corrosion resistant coating on aluminum alloy products. The coating is applied by an electrolytic treatment of the base material in a conductive acidic-aqueous bath that produces an adherent film of aluminum oxide. The oxide is formed in usable thicknesses because microscopic pores are present during the electrolytic oxidation process that allows access of the electrolyte to the base metal.

After producing the coating, the pores must be sealed or the protective capabilities of the coating would be seriously reduced. Sealing is normally accomplished by immersing the product in 180 to 200°F water for 30 minutes. This treatment hydrates the aluminum oxide, thereby changing its structure and causing the pores to close. One of the most commonly used tests for determining the presence of an anodic film is electrical conductivity. Since aluminum oxide is a dielectric, the surface of the product will not conduct if the coating is present. This test is rapid and convenient; however, it will not detect the lack of adequate sealing because the pore size is too small for electrical probes to be effective.

2. Test Setup

Test specimens were placed in 19-mm-diameter test tubes and then inserted into a 1-in.-diameter aluminum tube assembly. The tube was flared on each end and standard AN sleeves, nuts, and plugs were used as closures. The propellant was first treated with nitric oxide (NO) and then added to the test tube. The propellant was then allowed to flow inco the bottom of the aluminum tube to assure that at least 1/2 of the test specimen would be immersed in the liquid after boiloff of sufficient liquid to satisfy the vapor pressure demand at 135°C. Pressure was not measured during the test.

3. Selection of Materials

Selection of candidate materials was primarily influenced by four considerations: 1) Potential use for structural or special design applications; 2) Potential improvement of the basic resistance through application protective coatings; 3) Availability of the material; 4) Novelty of the material as related to initial testing.

Candidate materials were exposed to the propellant with two types of specimens: (1) prestressed specimens using the stressed configuration devised by NASA-Langley, and (2) unstressed specimens. Stressed specimens were loaded to 75% of yield strength.

Materials not stressed were tested in this manner because their inherent physical properties or their available form was not conducive to the preparation of the Langley type of stressed specimen. Also, some of the nonstressed materials would be used in airborne application as bearing or sealing surfaces and would never actually be stressed except with a minor shear load or in compression.

The following materials were selected for continuing compatibility evaluation with N_2O_4. Various groups of materials are presented and the reason for selecting each is discussed.

2021-T6 Aluminum, Chromic Acid Anodized, Stressed and Unstressed

2014-T6 Aluminum, Chromic Acid Anodized, Stressed and Unstressed

6061-T6 Aluminum, Chromic Acid Anodized, Stressed and Unstressed

2021-T6 Aluminum, Sulfuric Acid Anodized, Stressed and Unstressed

2014-T6 Aluminum, Sulfuric Acid Anodized, Stressed and Unstressed

6061-T6 Aluminum, Sulfuric Acid Anodized, Stressed and Unstressed

These alloys were tested during the early phases of this program. They were found to be acceptable for structural applications; however, they were attacked and suffered a few mils of intergranular corrosion and produced a small quantity of abrasive corrosion products. Limited testing was conducted on specimens that had been anodized. The Al_2O_3 coating seemed to afford a certain degree of protection. This possibility was pursued in the extension of the program. The alloys selected all possessed good structural strength and were considered typical of those that would be selected by the designer. Both chromic acid and sulfuric acid anodizing processes were tested because of the chemical, physical, and thickness differences of the coatings and the design restriction related to retaining residual sulfuric acid anodizing electrolyte in assembled units.

2024-T3, Clad, Not Stressed

2024-T3, Bare, Not Stressed

The primary purpose of this test was to ascertain the degree of protection afforded by the cladding of nearly pure aluminum on a high copper structural alloy. Previous tests with 1100-0 aluminum indicated that this type of material possessed greater corrosion resistance than the highly alloyed materials. The clad materials do not lend themselves to fusion welding, except when the cladding is removed in the weld zone. However if sufficient design margins were maintained in the major weld portion of the tankage, the small amount of attack and resultant corrosion products in the weld area might be acceptable.

430 Stainless Steel Alloy, Stressed and Unstressed

During the initial phase of testing, only 300 series alloys were tested because of their prominence in the construction of N_2O_4 propellant systems. Test results indicated that the high nickel content of these alloys was responsible for the creation of the amorphous, sticky substance as a corrosion product. The 430 alloy was selected as a representative sample of the 400 series stainless steels having low nickel content.

321 Stainless Steel, Chromium Plated, Stressed

This alloy exhibited properties of noncompatibility typical of all of the 300 series alloys. Since the presence of nickel in the alloy was considered the major cause of the corrosion product formation, a protective coating of 2 mils of chromium was applied. It was expected that a minor degree of attack would be sustained.

Titanium Alloy, 5Al - 2.5 Sn, Stressed and Unstressed

Titanium Alloy, 8Al - 1Mo, Stressed and Unstressed

These materials were included since only 6Al-4V was tested during the initial phase. This selection was intended to give the designer and manufacturing engineer a greater latitude in material selection.

Tantalum Sheet, Not Stressed

Unalloyed tantalum is extremely ductile and does not lend itself to stressed specimens. One of its primary uses, in commercial chemical applications, is in heating systems that must be exposed to hot acids. This material was tested as a possible source of screen material for a positive displacement device in low-gravity propulsion systems. Since it is extremely ductile, it could be easily drawn into wires and woven into screens.

Aluminum Oxide Ceramic

Beryllium Oxide Ceramic

Both of these materials will be completely unaffected by the N_2O_4 at 135°C. However, since no ceramics were tested earlier, and since a number of surprises have occurred, these materials were selected for test. Their potential use would be in close tolerance hard seats, sliding unit guides, or in drive mechanism subjected to compressive loading.

6061 Aluminum Screen, Chromic Acid Anodized

6061 Aluminum Screen, Sulfuric Acid Anodized

These materials were given further consideration for application as a positive displacement device in zero gravity. The purpose of the protective anodic coating was explained previously.

Beryllium, Not Stressed

Available samples of this material were such that the stressed specimen were not practical. The basic resistance to N_2O_4, at any temperature was questionable. Before loading the sample into a cest vessel, it was subjected to exposure to N_2O_4 at room temperature for 24 hr. No reaction was noted and it was accepted as a good test material. Although beryllium is difficult to fabricate, it possesses structural properties of interest to the designer. It is lighter and stronger than aluminum and has a modulus of elasticity of 40 million.

Tungsten, W-2, Not Stressed

This material is extremely brittle and does not lend itself to the Langley type of stressed specimen. It will withstand extremely high temperatures and possesses excellent resistance to wear by abrasion. Its application in an engine module would be in areas where a high degree of abrasion would occur or where high temperatures are expected. Because of its brittleness, structural applications should be made where loading is primarily compressive.

Cobalt (L605), Stressed and Unstressed

This alloy is a high chromic-nickel cobalt-based alloy containing 15% tungsten. Its primary aerospace use is in construction of hardware that will be exposed to high temperatures, e.g., the engine compartment. This alloy could have application in engine

components that would be exposed to the propellant during dry heat sterilization and exposed to high temperatures during engine firing. If found compatible, cobalt could also replace hardware for general propulsion tankage construction as a substitute for the 300 series stainless steels.

Columbium Alloy DP-14

Columbium Alloy CB752, Stressed and Unstressed

These alloys are low strength, highly ductile materials that exhibit a high degree of resistance to nitric acid. They could be easily woven into screens for use in positive displacement assemblies for low-gravity propellant expulsion.

AMS 5538 - Cyclops, Stressed and Unstressed

This is a precipitation hardened stainless steel which exhibits high strength in the annealed condition, i.e., 65,000 YTS and 120,000 UTS. It could serve in a variety of structural applications for tankage, tubing, and components. It also possesses good structural properties at high temperatures.

HY-140 Steel Plate, Not Stressed

This material was not stressed because its available form was plate and was not practical for use as a Langley-type specimen. It is a low alloyed high-strength steel that retains almost 100% of its strength in weld areas. It has a 140,000 psi YTS and excellent fracture toughness. HY-140 is currently being given consideration as a structural material for tankage for new USAF weapon systems.

Austenitic Stainless Steel Alloy 21-6-9, Stressed and Unstressed

This is a high chromium content (21%), high manganese (9%) stainless steel alloy. It has high strength in the annealed condition and can be strain hardened to 180,000 psi YTS. It would be an excellent structural material for propulsion tanks, liners, and fittings. It has good welding and forming characteristics.

TZM Titanium-Zirconium-Molybdenum Alloy

This material is a molybdenum based alloy containing titanium and zirconium. Its normal use is in high temperature structures.

4. Test Results

The general results of the materials exposure may be summarized as follows:

1) Anodic coating of aluminum alloys can ensure almost 100% protection to these materials;

2) Commercially pure aluminum cladding of structural aluminum alloys provides 100% protection with a very slight amount of corrosion products formed. The formation of corrosion products was so small the material may be classified as compatible;

3) Tantallum and columbium were unaffected by the propellant. Both of these materials are highly ductile and would be capable of producing high quality screens for positive displacement devices;

4) Chromium plating stainless steels afford excellent protection to the base material although only 321 stainless steel was tested. This protection could be afforded to any metallic material;

5) L-605 cobalt alloy sustained weld surface attack and may be considered marginally compatible. It in no way resembled the poor corrosion resistance of the high nickel ferrous alloys;

Table V-1 presents the compatibility results in summary form for easy reference.

Comments on the individual material specimens present the detailed observations. Where appropriate, photomicrographs were examined to aid in the specimen evaluation.

a. Aluminums

2014-T6 Aluminum, Anodized with Chromic Acid - No observable attack. Anodic coating was intact, as determined by electrical measurements which showed that the surface of the specimen was not conductive. Figure V-1 shows a photomicrograph that is representative of the degree of protection afforded aluminum by the anodic coating produced by chromic acid.

2014-T6 Aluminum Anodized with Sulfuric Acid - No observable attack. Anodic coating was intact as determined by electrical testing. Figure V-2 is a photomicrograph that demonstrates the protection afforded.

Table V-1 Materials Compatibility Exposed to N_2O_4 at 135°C for 600 Hours

	Material	Results*
1.	2014-T6 Aluminum, Chromic Acid Anodized	C
2.	2014-T6 Aluminum, Sulfuric Acid Anodized	C
3.	6061-T6 Aluminum, Chromic Acid Anodized	C
4.	6061-T6 Aluminum, Sulfuric Acid Anodized	C
5.	2021-T6 Aluminum, Chromic Acid Anodized	N/A
6.	2021-T6 Aluminum, Sulfuric Acid Anodized	C
7.	6061 Aluminum, Screen Chromic Acid Anodized	C
8.	6061 Aluminum, Screen Sulfuric Acid Anodized	N/A
9.	2024-T3 Aluminum, Pure Aluminum Clad	C
10.	2024-T3 Aluminum, Clad Stripped	NC
11.	430 Stainless Steel	C
12.	321 Stainless Steel, Chrome Plated	MC
13.	AMS 5538 Stainless Steel	MC
14.	21-6-9 Stainless Steel	MC
15.	HY-140 Steel	C
16.	Titanium 5Aℓ-2.5 Sn	C
17.	Titanium 8Aℓ-1 Mo	C
18.	Beryllium	C
19.	Columbium DP14	C
20.	Columbium CB752	C
21.	Tantalum, Pure	C
22.	Tungsten, Pure	C
23.	TZM Titanium-Zirconium-Molybdenum	MC
24.	L-605 Cobalt	MC
25.	Beryllium Oxide Ceramic	C
26.	Aluminum Oxide Ceramic	C

*C - compatible; MC - marginally compatible; NC - not compatible; and N/A - not available, specimen improperly prepared.

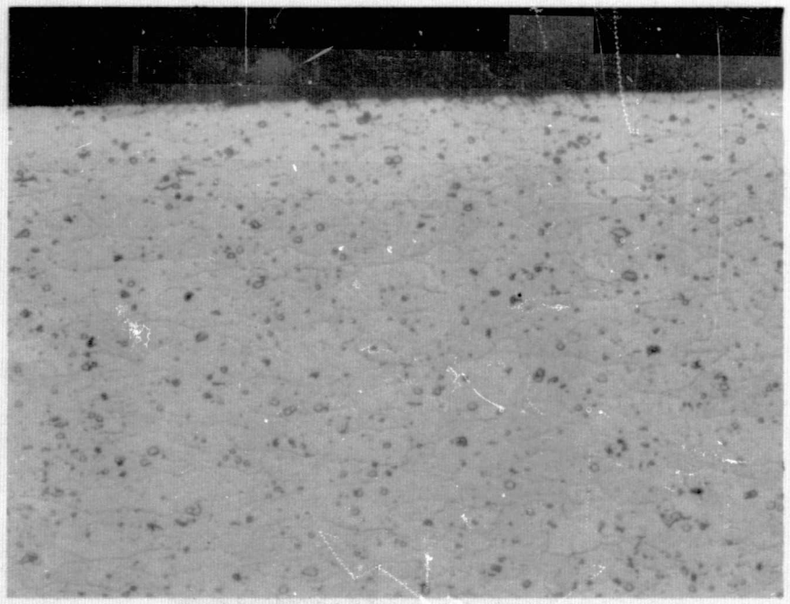

(a) Chromic Acid Anodized

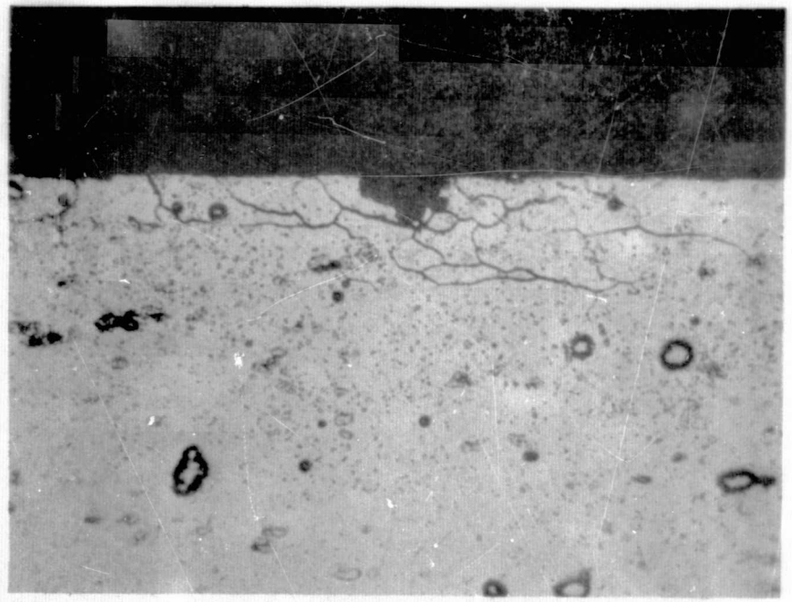

(b) Bare Metal

Note: No attack is noted on the chromic acid anodized aluminum.

Fig. V-1 Aluminum (2014-T6) after Exposure to N_2O_4 for 600 Hours at 135°C (200x)

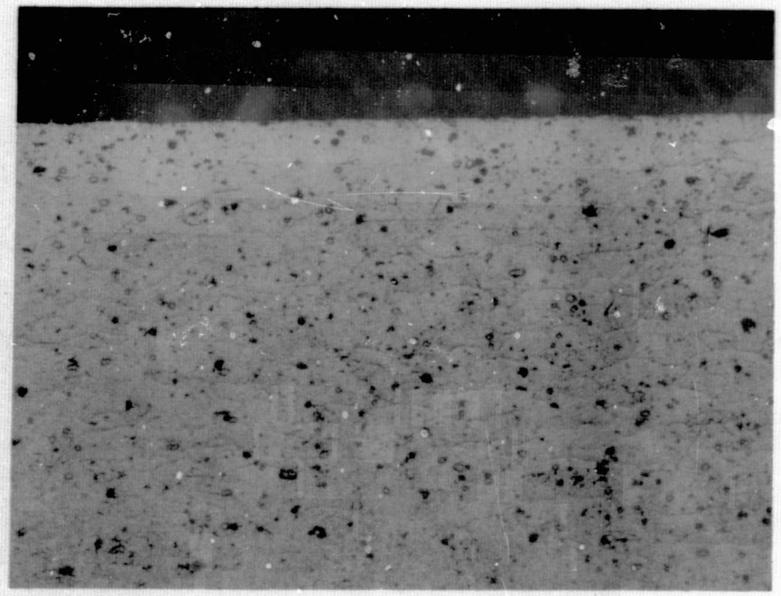

(a) Sulfuric Acid Anodize

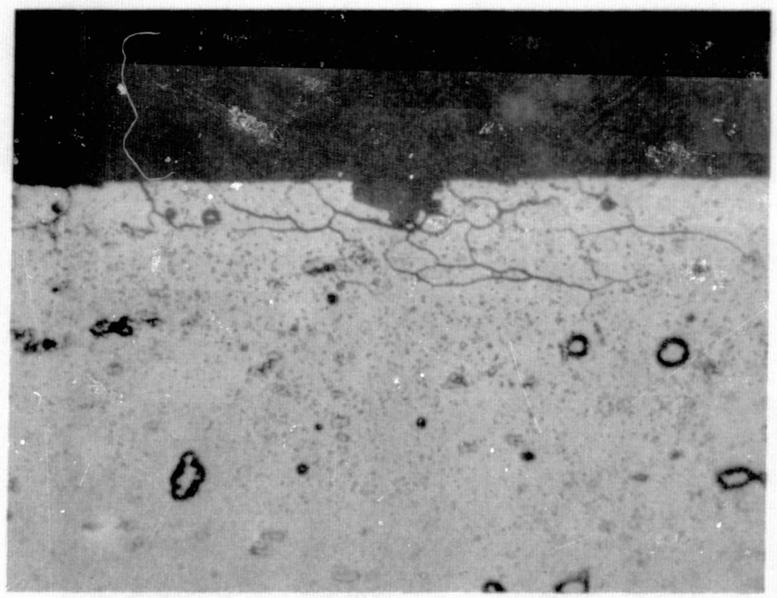

(b) Bare Metal

Note: No attack is noted on the sulfuric acid anodized aluminum.

Fig. V-2 Aluminum (2014-T6) after Exposure to N_2O_4 for 600 Hours at 135°C (200x)

6061-T6 Aluminum Anodized with Chromic Acid - No observable attack. Anodic coating was intact.

6061-T6 Aluminum Anodized with Sulfuric Acid - No observable attack. Anodic coating was intact.

2021-T6 Aluminum Anodized with Chromic Acid - This specimen and the glass container had a light coating of an extremely fine, white powder. This indicated that a minute amount of the aluminum base material had been removed. Although the anodic coating was found to have remained (this was determined by conductivity measurements) it appears that the hot water seal was inadequate. This seal is performed subsequent to anodizing in order to close the pores formed during the process through hydration of the oxide film. It also points out the importance of an adequate seal for complete protection of the base metal. Since this did not occur with the other wrought alloy specimens, it may be concluded that inadequate processing was the cause of the attack.

2021-T6 Aluminum Anodized with Sulfuric Acid - No observable attack. Anodic coating was intact.

6061 Aluminum Screen Anodized with Chromic Acid - No observable attack was found. Anodic coating was intact. See Fig. V-3 for a microsection of this specimen.

6061 Aluminum Screen Anodized with Sulfuric Acid - A light, powdery residue was found on the specimen and in the glass container indicating the same type of attack and incomplete processing as was found with the chromic acid anodized 2021-T6 wrought sample. Here again, the surface was not electrically conductive.

2024-T3 Aluminum with a Commercially Pure Aluminum Clad - Degree of attack was not significant. A minute amount of an externally fine powder was on the specimen surface. Figure V-4 demonstrates the low degree of attack and the lack of any penetration of the cladding.

2024-T3 Aluminum with Cladding Stripped before Test - Reacted typically of highly alloyed, unprotected aluminum structural alloys. This resulted in intergranular attack and formation of corrosion products.

Note: The chromic acid anodized specimen sustained no attack.

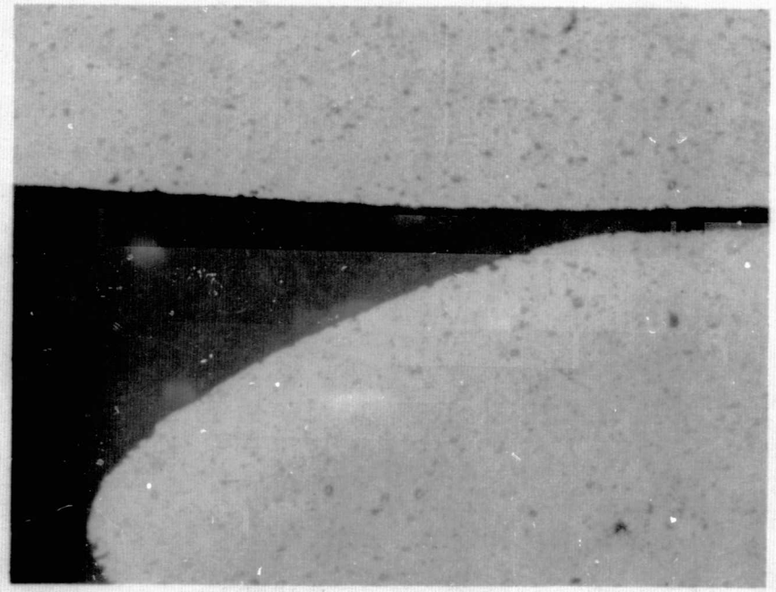

(a) 6061 Alloy Chromic Acid Anodized

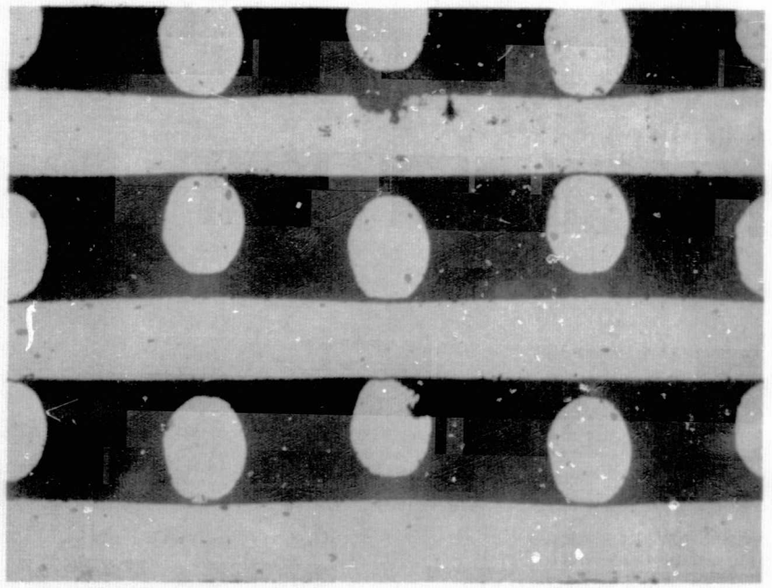

(b) 5056 Alloy Bare Metal

Fig. V-3 Aluminum Screen after Exposure to N_2O_4 for 600 Hours at 135°C (200x)

Note: Surface is free of pits; there was no penetration of the clad coating

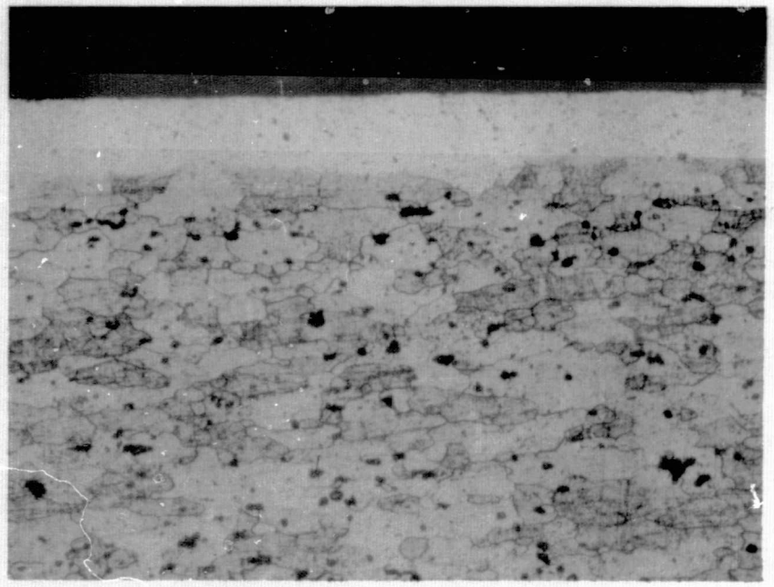

Fig. V-4 Aluminum (2024-T3) Clad with Pure Aluminum after Exposure to N_2O_4 for 600 Hours at 135°C (200x)

b. Steels - Stainless steels were tested further. As may be seen in the results of initial tests conducted during this contract, all candidate 300 series stainless steels were found to be unacceptable for use in the specified environment because of the formation of large quantities of a thick, viscous material. Chemical assay of this product showed that its elemental composition was the same as that of the test specimen. The presence of a relatively high nickel content was suspected to cause the reaction. This series of tests were conducted to gain additional data related to the nickel content effect, the value of a protective coating, and to stainless steels other than the common 300 series alloys tested during the initial phase of this contract. Results are as follows.

430 Stainless Steel - This alloy sustained a minor degree of attack that resulted in superficial darkening of the specimen surface. There was no formation of any of the viscous corrosion product or of intergranular corrosion that was typical of the 300 series alloys. The surface darkening was primarily found in areas that were freshly sheared or had recently been shot peened. Since the specimen had been passivated before specimen preparation, and not after, this indicates that the specimen was more active in the freshly worked areas. Photomicrographs were taken of a passivated surface (Fig. V-5) and a shot peened surface (Fig. V-6). As may be seen, no observable chemical attack existed on either area. The rougher appearance of Fig. V-6 is the result of the shot peening. This alloy may, for all practical purposes, be considered inert to the propellant sterilization environment.

321 Stainless Steel, Chromium Plated - A light attack was sustained with resultant formation of a minute amount of viscous corrosion product. The amount of the product formed was less than 1% of that formed when bare 321 stainless steel was exposed to N_2O_4 during the sterilization cycle. Ordinarily, chromium plating is a poor protective coating against corrosion because of microscopic porosity inherent to this coating. This porosity apparently allowed the small degree of attack to take place. There are proprietary processes available which produce a crack-free chromium plating. Application of this type of coating could be of significant value in protecting the 300 series stainless steel alloys. Figure V-7 illustrates the degree of protection provided by the standard plating process.

Fig. V-5 430 Stainless Steel Passivated Surface

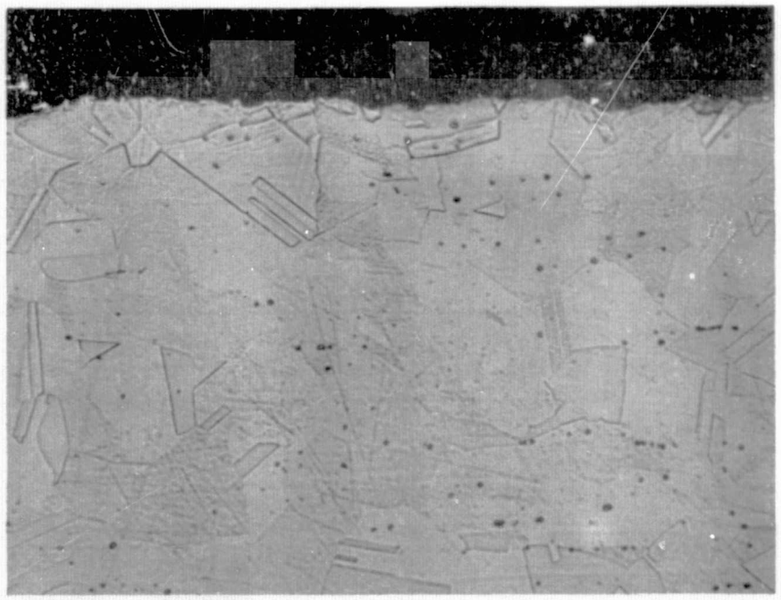

Fig. V-6 430 Stainless Steel Freshly Peened Surface

Note: There was no evidence of intergranular attack or pitting in either photograph. Surface roughness shown in Fig. V-6 was the result of shot peening.

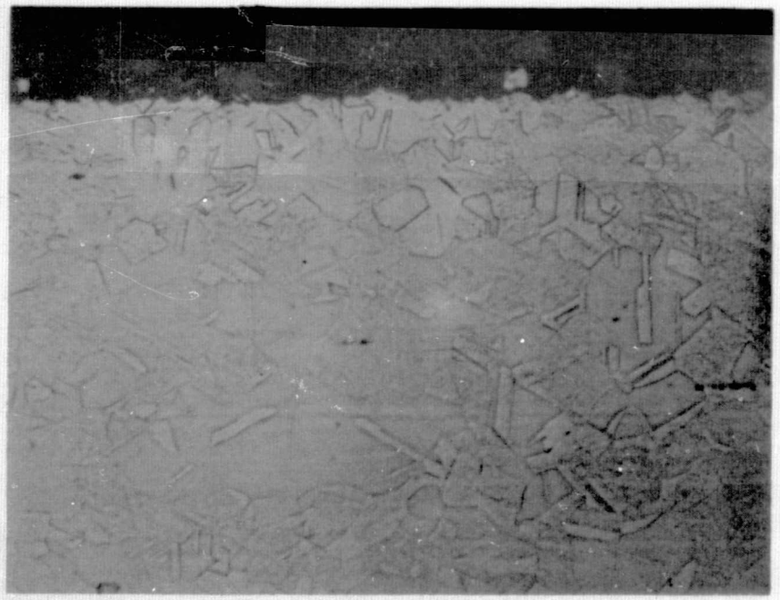

(a) Chrome Plated

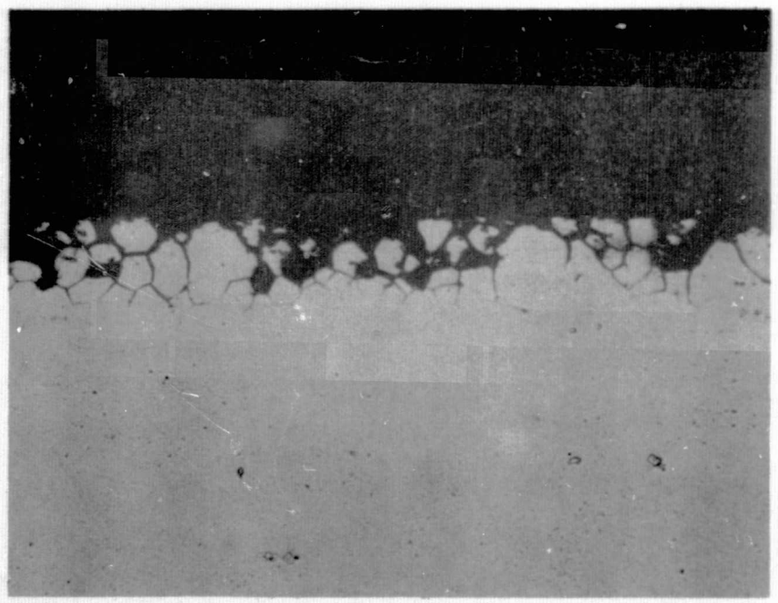

(b) Bare Metal

Note: The chrome plated specimen was not attacked. The plating is shown as a dark surface in Fig. V-7 (a).

Fig. V-7 Stainless Steel (321 series) after Exposure to N_2O_4 for 600 Hours at 135°C (200x)

AMS 5538 Cyclops, Stainless Steel Alloy - Surface attack was noted with resultant formation of a few beads of the viscous corrosion product and a general roughening of the specimen surface. This material was affected much less than were the bare 300 series alloys. Figure V-8 illustrates the degree of attack.

21-6-9 Stainless Steel Alloy - Surface attack was sustained with formation of a few beads of the typical corrosion product. This material reacted in a manner similar to that of AMS 5538. Figure V-9 illustrates the minor degree of attack as well of the lack of significant intergranular corrosion.

HY-140 (HY represents high yield strength of 140 ksi) - To further pursue the idea that nickel may be a major contributor to the attack on ferrous alloys, a low alloyed material possessing excellent structural properties was tested. This specimen was polished to a mirror finish before the test. On removal from the propellant, this finish was unaffected. HY-140 demonstrated greater corrosion resistance than 6Aℓ-4V titanium or any ferrous based alloy tested.

c. Titaniums - Since the 6Aℓ-4V titanium had exhibited superior corrosion resistance to that of any alloy tested in the first series of this contract, it was determined that additional representative alloys of titanium be evaluated to establish whether this characteristic was typical of titanium. Results were as follows.

5Aℓ-2.5Sn Titanium Alloy - Light surface attack was found with the formation of an iridescent film that is typical of that formed on 6Aℓ-4V titanium. Both alloys are considered comparable in resistance to attack by the propellant. Figure V-10 demonstrates this alloy's high degree of compatibility.

8Aℓ-1Mo Titanium Alloy - This alloy reacted identically as that of 5Aℓ-2.5Sn.

d. Miscellaneous Materials - Another series of materials were selected for test because they were unique in relation to those previously tested. Results were as follows.

Beryllium - This metal was completely unaffected by the propellant. Initially, it was suspected that its exposure to N_2O_4 might cause a sufficient rate of reaction that extreme pressure would result in a closed vessel. Therefore, preliminary testing was conducted in an open beaker containing 100 cc of N_2O_4 and about 1 cu in. of beryllium. This test container was allowed to vent in contact with air until all the propellant had evaporated (about 3 hr). No reaction was noted. This material may be considered inert to the propellant.

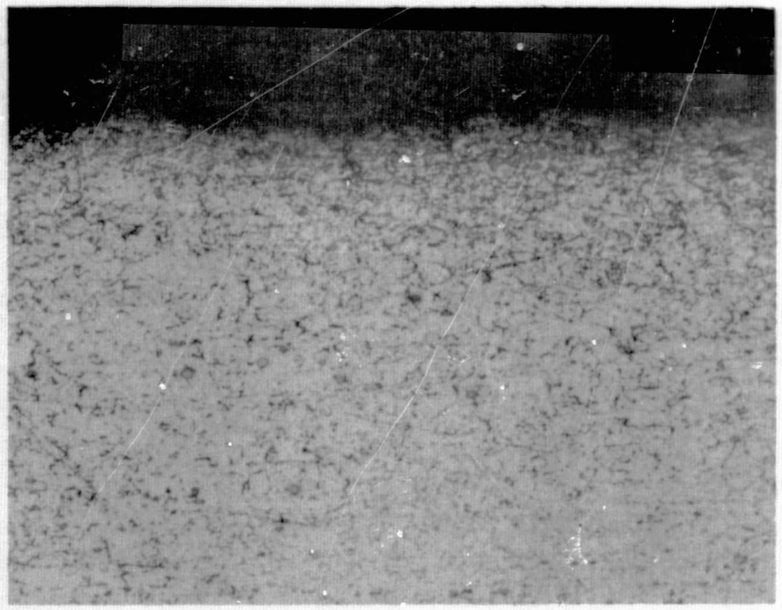

Note: Surface attack is evidenced by small pits. No significant intergranular attack is apparent.

Fig. V-8 Stainless Steel (AMS 5538) after Exposure to N_2O_4 for 600 Hours at 135°C (200x)

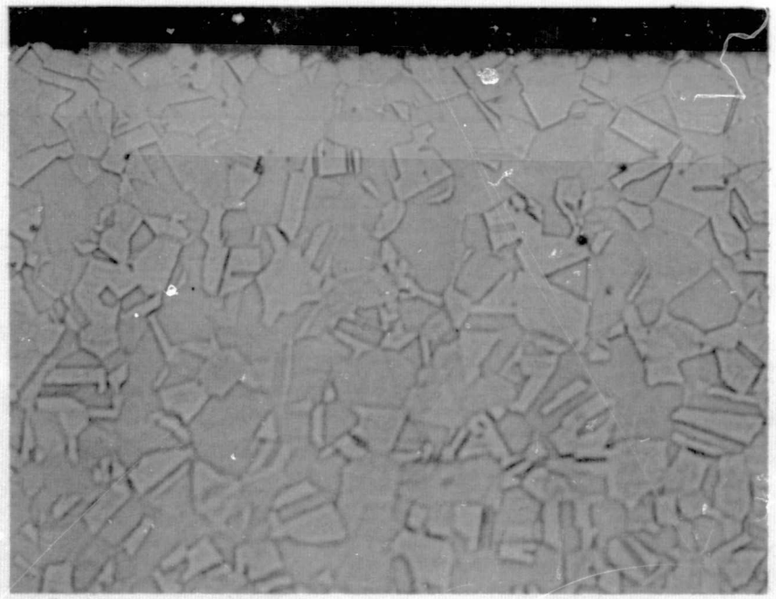

Note:	Surface is roughened by pitting. Some intergranular corrosion is observable. Structural strength not affected.

Fig. V-9 Stainless Steel (21-6-9) after Exposure to N_2O_4 for 600 Hours at 135°C (200x)

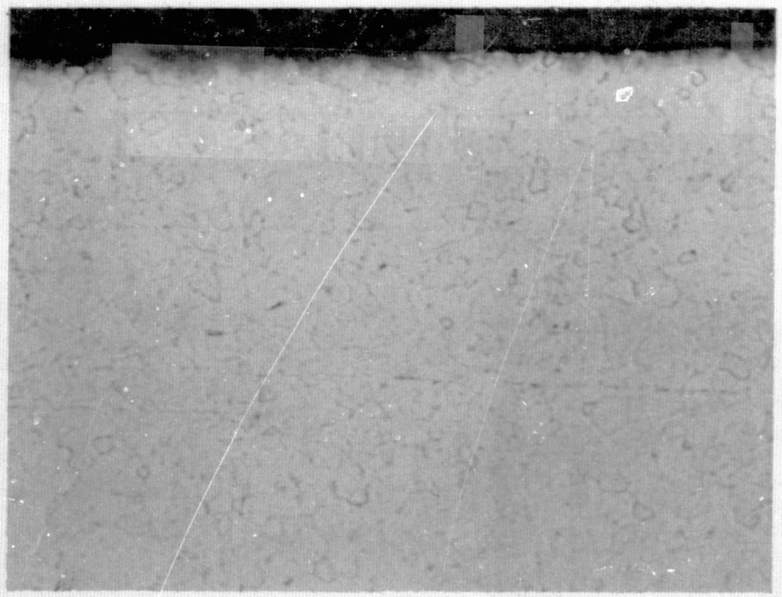

(a) 5Aℓ-2.5 Sn Alloy

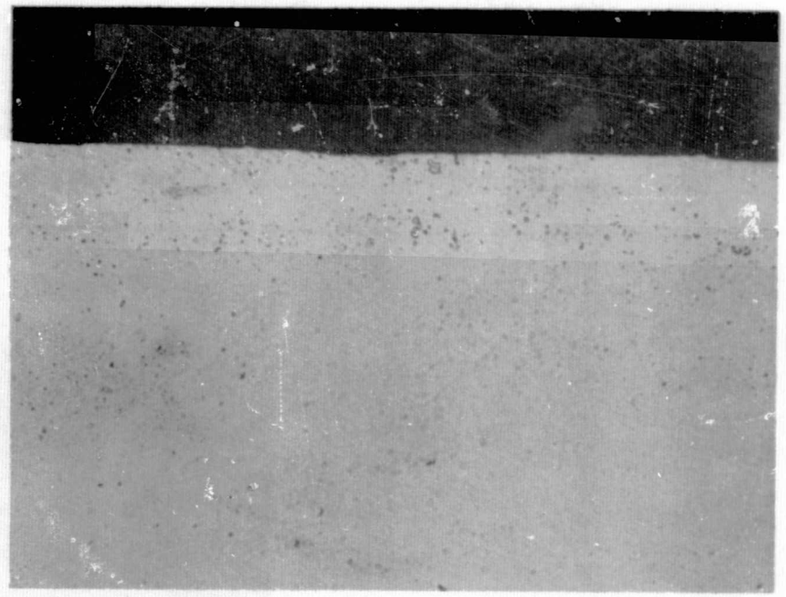

(b) 6Aℓ-4V Alloy

Note: No evidence of attack of either alloy.

Fig. V-10 Titanium Alloys after Exposure to N_2O_4 for 600 Hours at 135°C (200x)

Columbium Alloy, DP14 - Light surface attack with attendant discoloration was noted. No loose corrosion products were formed. Figure V-11 illustrates the degree of corrosion resistance that this alloy possesses.

Columbium Alloy CB752 - This alloy reacted identically as the DP14 discussed above.

Tantallum, Commercially Pure - No attack occurred. Tantallum is inert to the propellant.

Tungsten, Commercially Pure - No attack occurred.

TZM (Titanium-Zirconium-Molybdenum) - A light surface attack with the formation of smut and some surface roughing was observed.

L-605 Cobalt Super Alloy - Surface attack with formation of a white, loosely adherent corrosion product was noted. This alloy was tested, primarily because of its chemical similarity to nickel. Resultant corrosion products indicated cobalt behaves considerably different than nickel in the sterilization environment with N_2O_4. Figure V-12 shows a photomicrograph of this material's surface after testing.

Beryllium Oxide Ceramic - This material sustained no chemical attack and no increase in weight as the result of absorption. It is inert to the propellant.

Aluminum Oxide Ceramic - This material sustained no chemical attack and no increase in weight as the result of absorption. It is inert to the propellant.

5. Long-Term Storage Testing

Part I of the final report presents the results of the fuel tank storage tests after one year ambient exposure after sterilization. There was no degradation of the fuel or the materials. Similarly, the oxidizer tanks tests showed no significant attack on any of the materials of construction and the TFE/FEP laminate material suffered no degradation. The oxidizer tanks had been stored for 13 months at ambient conditions after being exposed to 600 hr of heat sterilization.

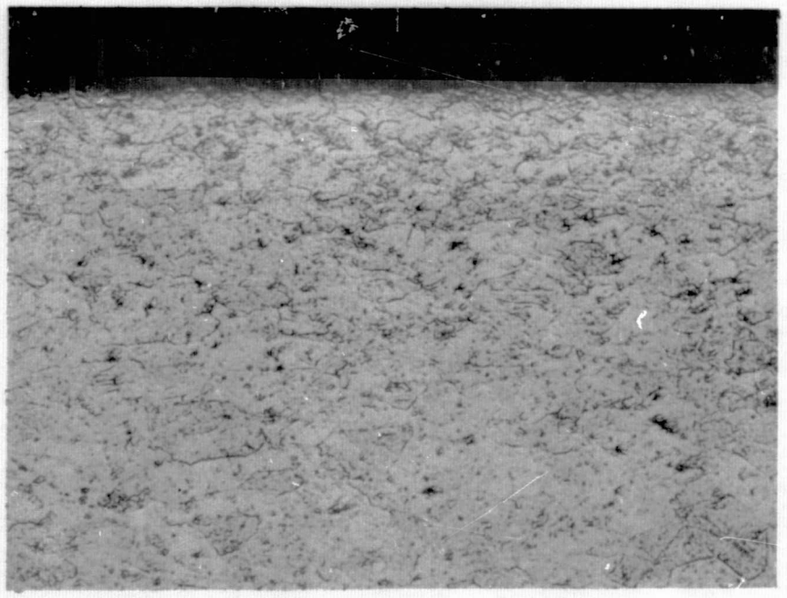

Note: No evidence of surface attack or intergranular corrosion observable. The light attack seen during surface examination was too small to be seen at 200x magnification.

Fig. V-11 Columbium (DP14) after Exposure to N_2O_4 for 600 Hours at 135°C (200x)

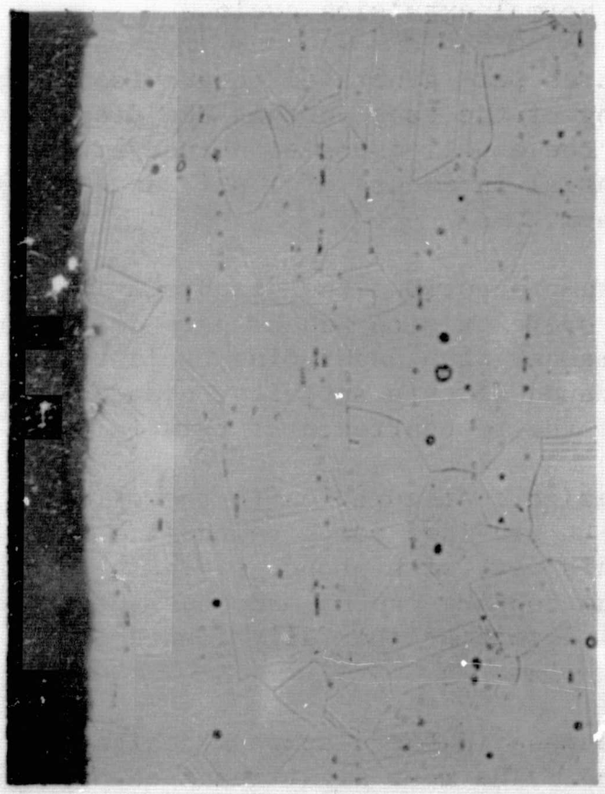

Note: Some minute pitting of the surface is in evidence.
No intergranular corrosion occurred.

Fig. V-12 Cobalt (L-605) after Exposure to N_2O_4 for 600 Hours at 135°C (200x)

B. SYSTEM DESIGN MODIFICATIONS

1. Oxidizer Tank and Diaphragm

a. Description of Changes - Examination of the oxidizer tank following the initial module firing revealed a rupture of the Teflon expulsion diaphragm. The overexpulsion was due to the particular design of diaphragm installation. This design required that the diaphragm be mounted 0.8 in. off center to prevent damage to the diaphragm when making the final girth weld of the tank hemispheres (see Fig. V-13). As a result of this installation the diaphragm did not touch the wall of the lower hemisphere when folded through during a normal expulsion cycle.

Detailed procedures were generated to provide for propellant filling and handling of the tank so that the diaphragm was never folded through to the expelled position inadvertantly or that a pressure differential in excess of 1 psi was never generated across the diaphragm.

In spite of these precautions the diaphragm in the module was ruptured because of overexpulsion and a spare diaphragm was destroyed in a similar manner when undergoing cycle tests as part of another program. Because of this activity, changes were made to the design to prevent the reoccurrence of this failure.

The resulting design configuration to the oxidizer tank is shown in Fig. V-14. It provides for a centerline installation of the diaphragm. In this way, with proper sizing of tank and diaphragm, a line-to-line contact can be made between the diaphragm and the tank wall in either the fully loaded or the fully expelled position.

Several changes were made in the diaphragm design when the diaphragms were reordered. The most significant change was a resizing of the diaphragm to prevent the apparent oversize found on the initial order. The diaphragm had to be squeezed in on the initial assembly by approximately 0.125 in. This resulted in lines of "mud cracking" when examined following sterilization. To overcome this the size of the diaphragm was reduced by 2%, allowing the unit to stretch into position when exposed to the high temperature and vapor pressure experienced during sterilization. As a result the radius of the diaphragm was reduced to 8.085 in., allowing for a 0.165-in. stretch.

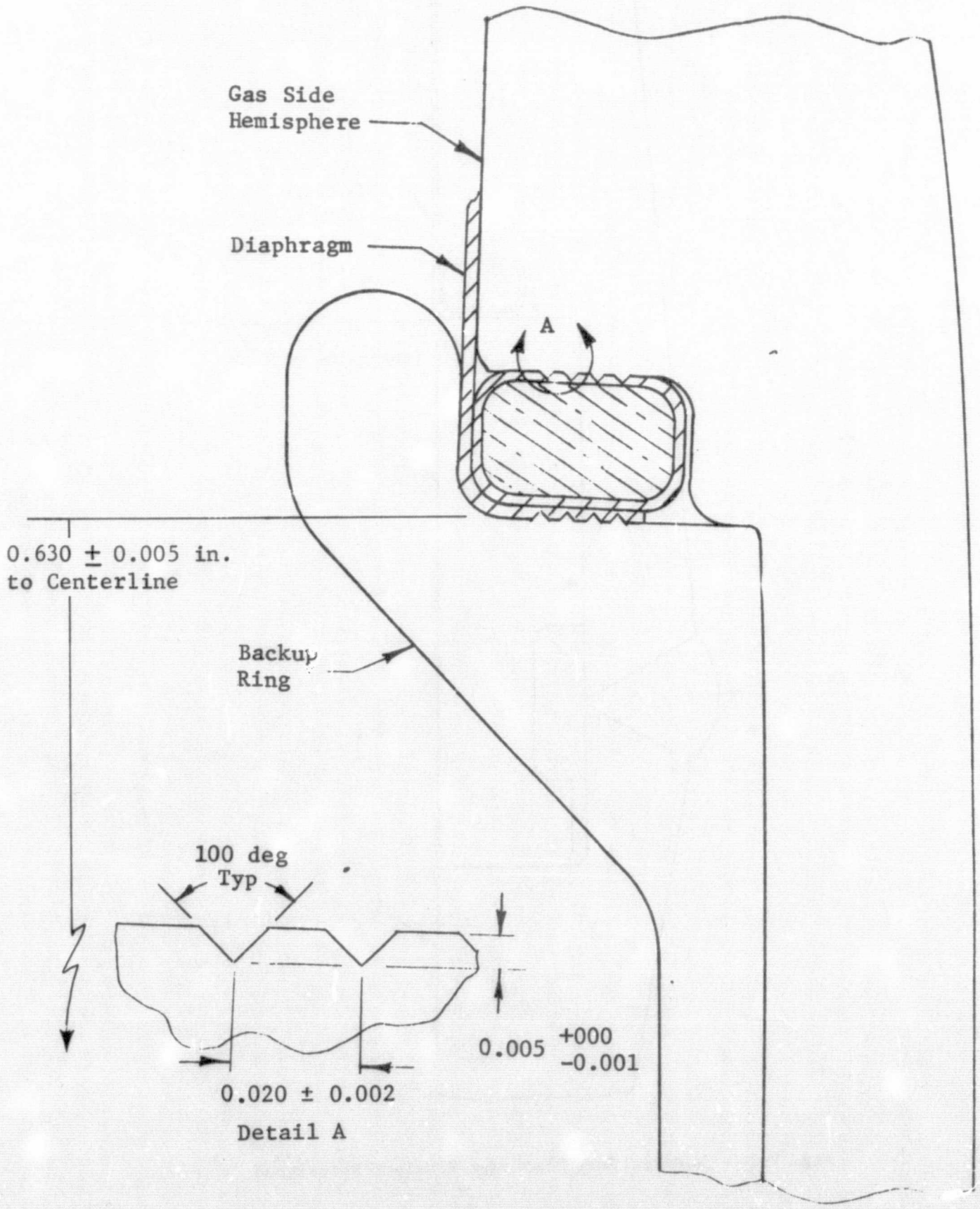

Fig. V-13 Oxidizer Tank, Original Seal Joint Design

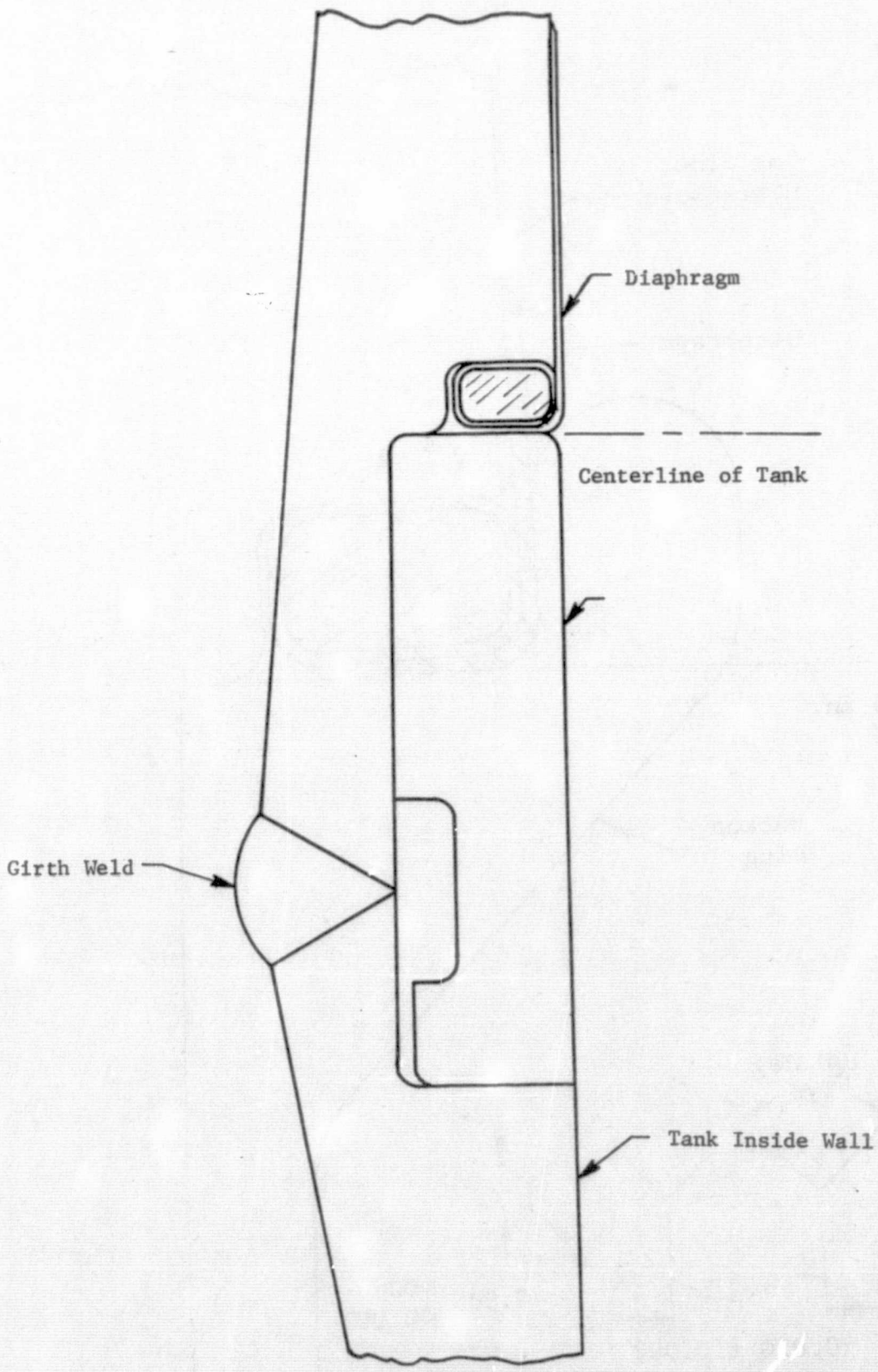

Fig. V-14 Oxidizer Tank Diaphragm Retainer Redesigned

Two other changes were made in the design. The apex doubler was reduced in thickness from 0.035 in. to 0.020 in., maximum, and the method of formation was changed. Originally a doubler was fused in place while the new design called for additional sprays of Teflon FEP on the outside surface. This change was incorporated to eliminate the relaxation of the integral doubler that resulted in a highly stressed area and leak in the original component test.

A minor change was made in the coating material of the flange ring by substituting a codispersion Teflon for the TFE/FEP laminate. This change provided for better process control of the coating application. Figure V-15 shows the diaphragm in the approved configuration.

b. Fabrication and Assembly

Diaphragms - During the fabrication of the diaphragms some difficulty was experienced in obtaining a heat fusion of the membrane to the flange ring. The ring was coated with codispersion Teflon with a thin coating of FEP applied as the final spray on the bottom of the ring. This was to provide a positive heat seal between the codispersion ring and the laminated membrane. The sealing of the first diaphragm was extremely difficult and the heat sealing operation was repeated several times before a leaktight seal was obtained. Some blistering of the seal area was evident. There was no established criteria for the inspection and acceptance of the heat seal area. As a result, the diaphragms were shipped to Denver so that the heat seal area could be reworked by hand stoning the surfaces for a smoother finish. Table V-2 presents the data before and after rework. The drawing value for the total flange thickness was 0.110 to 0.112 in. The delivered and reworked units were slightly thicker than this value; therefore some unevenness could be accepted and still effect a good seal. On the basis of these results S/N 102 was assigned to the module build and S/N 101 was assigned to the component tank. Figure V-16 is a photograph of the seal area blistering. As explained later this seal provided an effective seal.

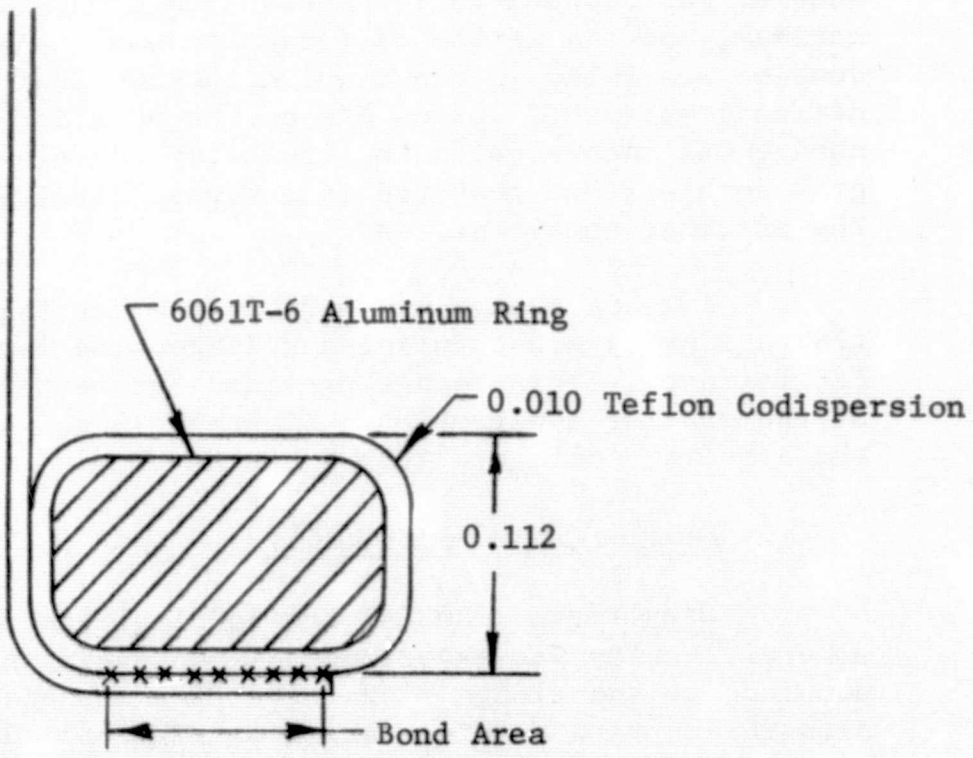

Cross Section A

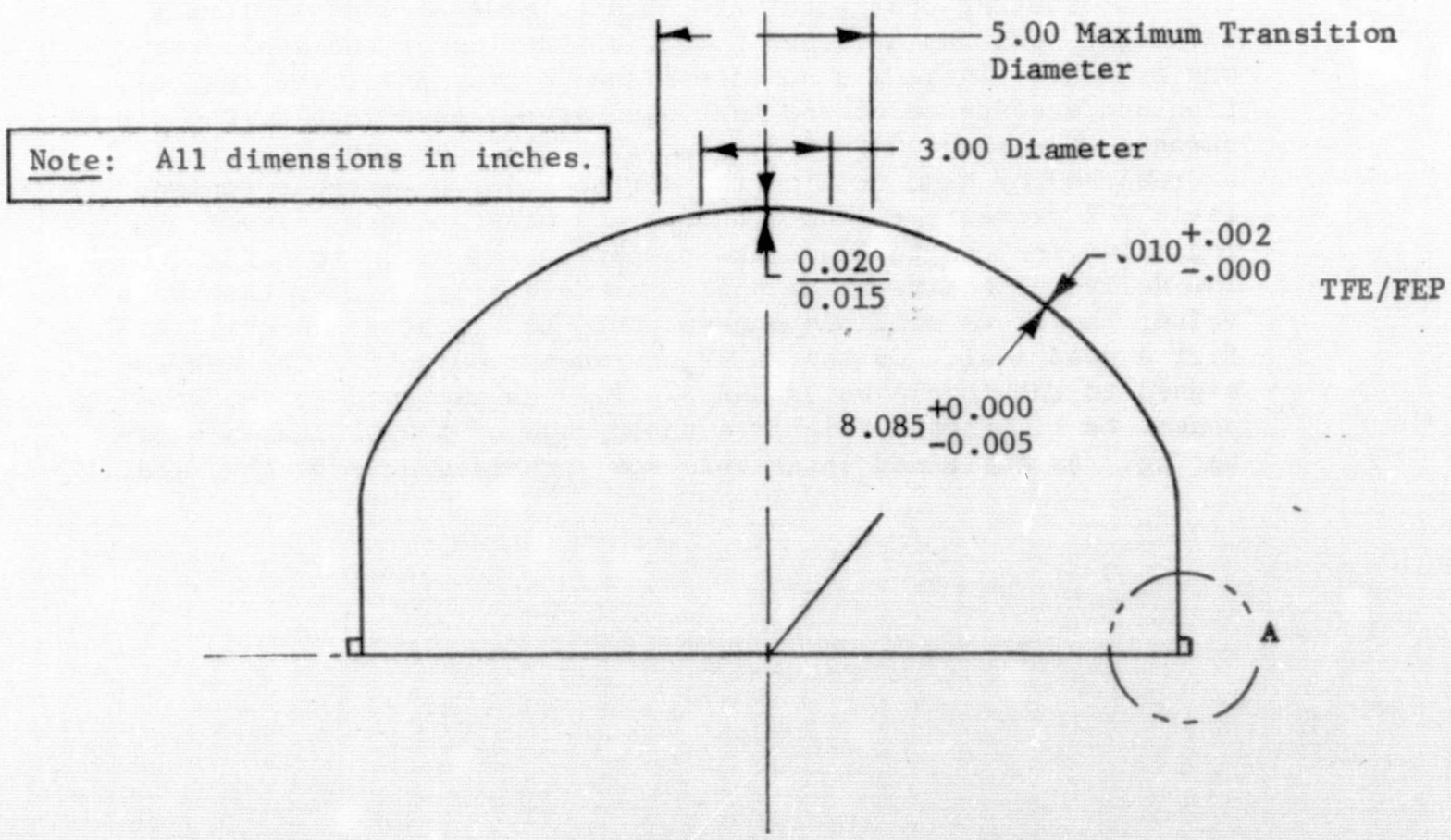

Fig. V-15 Oxidizer Tank Diaphragm Design

Table V-2 Diaphragm Rim Thickness

Station	S/N 101		S/N 102	
	As Received	After Rework	As Received	After Rework
1	0.1145	0.1145	0.115	0.114
2	0.116	0.115	0.114	0.113
3	0.116	0.115	0.1145	0.114
4	0.1155	0.115	0.115	0.114
5	0.117	0.1155	0.114	0.114
6	0.1152	0.115	0.115	0.114
7	0.115	0.115	0.115	0.114
8	0.1145	0.1145	0.1155	0.114
9	0.1155	0.115	0.1165	0.114
10	0.1148	0.1148	0.1163	0.114
11	0.114	0.114	0.1163	0.114
12	0.1145	0.1145	0.115	0.114
13	0.1142	0.1142	0.112	0.112
14	0.1152	0.115	0.113	0.113
15	0.1155	0.115	0.1138	0.1135
16	0.116	0.1155	0.114	0.114
17	0.1155	0.115	0.115	0.114
18	0.117	0.1155	0.116	0.114
19	0.1162	0.1155	0.116	0.114
20	0.1152	0.1152	0.116	0.114
21	0.115	0.115	0.115	0.114
Max.	0.117	0.1155	0.1165	0.114
Min.	0.114	0.114	0.112	0.112

Fig. V-16 Diaphragm Seal

Oxidizer Tanks - During the final assembly of the oxidizer tanks a major problem was encountered. The Teflon diaphragm to be installed inside the oxidizer tank was purposely designed 2% undersize as described above. When the final steps were taken to seat the diaphragm inside the hemisphere wall the diaphragm took a permanent set so that the minimum section thickness was less than one-third its original value. When the remaining diaphragm was installed in the tank in a heated condition, it survived the initial stretching operations and leak check; however, preliminary checks before formal acceptance testing indicated a severe leak in the diaphragm. Subsequent tank disassembly showed the substituted unit had a small hole approximately 1/16 in. in its greatest dimension.

The failure was characterized by stretching of the diaphragm around approximately 75% of the circumference as indicated by a white streak. In the one case a small hole developed, while in the original unit a hole did not develop. Figure V-17 shows the general arrangement of the propellant tank weld area, and the point of failure of the diaphragm. The photographs of the failures are shown in Fig. V-18. The assembly steps leading to the failure of both diaphragms are described in the following paragraphs.

Diaphragm S/N 102 was selected for assembly into the system tank, or module tank because the flange-to-membrane seal appeared to be in a better condition. The diaphragm was placed in the upper tank hemisphere and fitted with the retainer ring to hold it in place. This provided a vacuumtight seal. A vacuum was then drawn behind the diaphragm to stretch it into place. When a vacuum of 20 in. Hg was reached the diaphragm began to stretch beyond the elastic limit around the girth area as indicated by a white coloration.

The assembly process was immediately stopped and the diaphragm removed. The wall thickness of the Teflon diaphragm was determined to be 0.003 in. as compared to the nominal figure of 0.010 in.

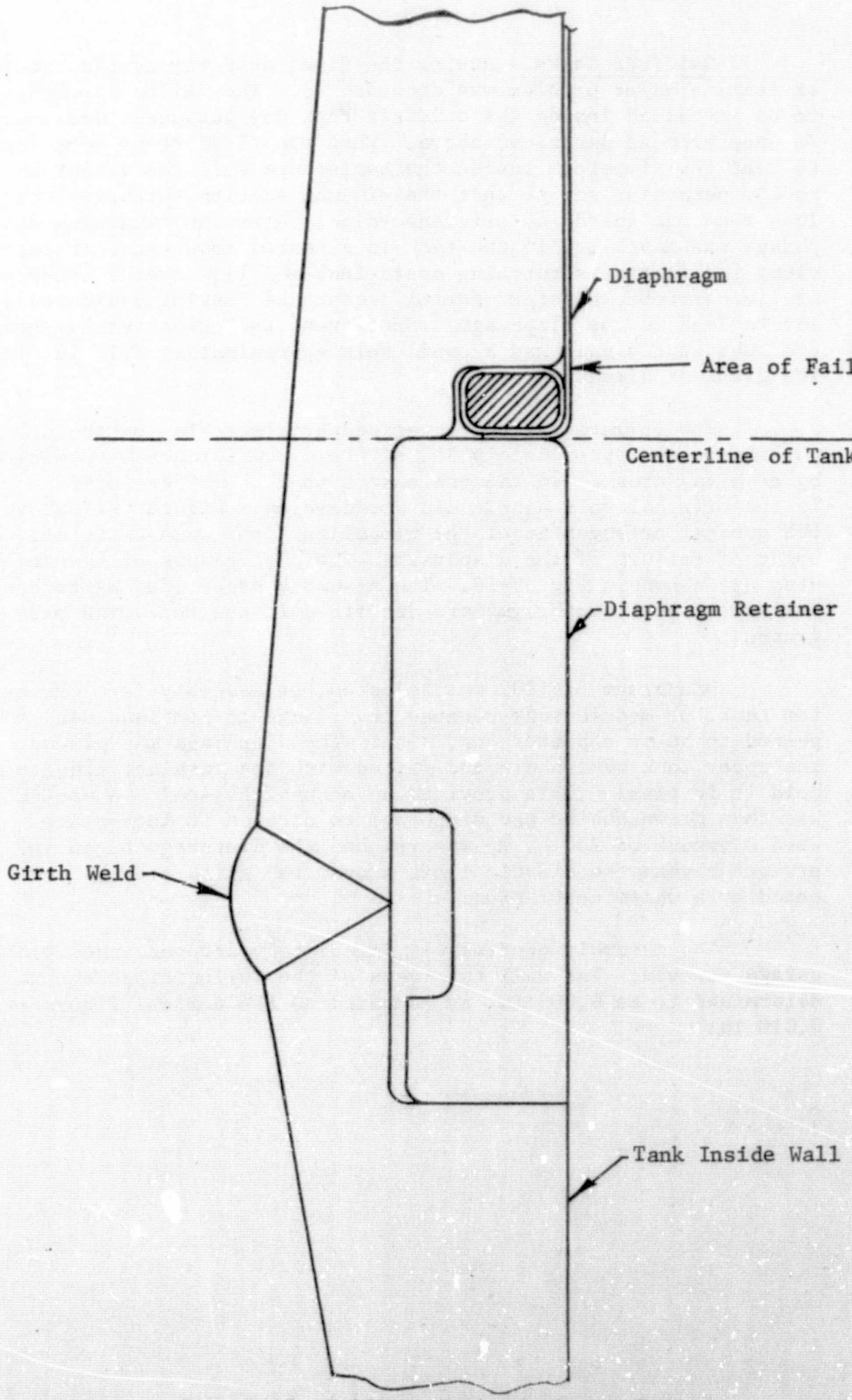

Fig. V-17 Oxidizer Tank Diaphragm Failure

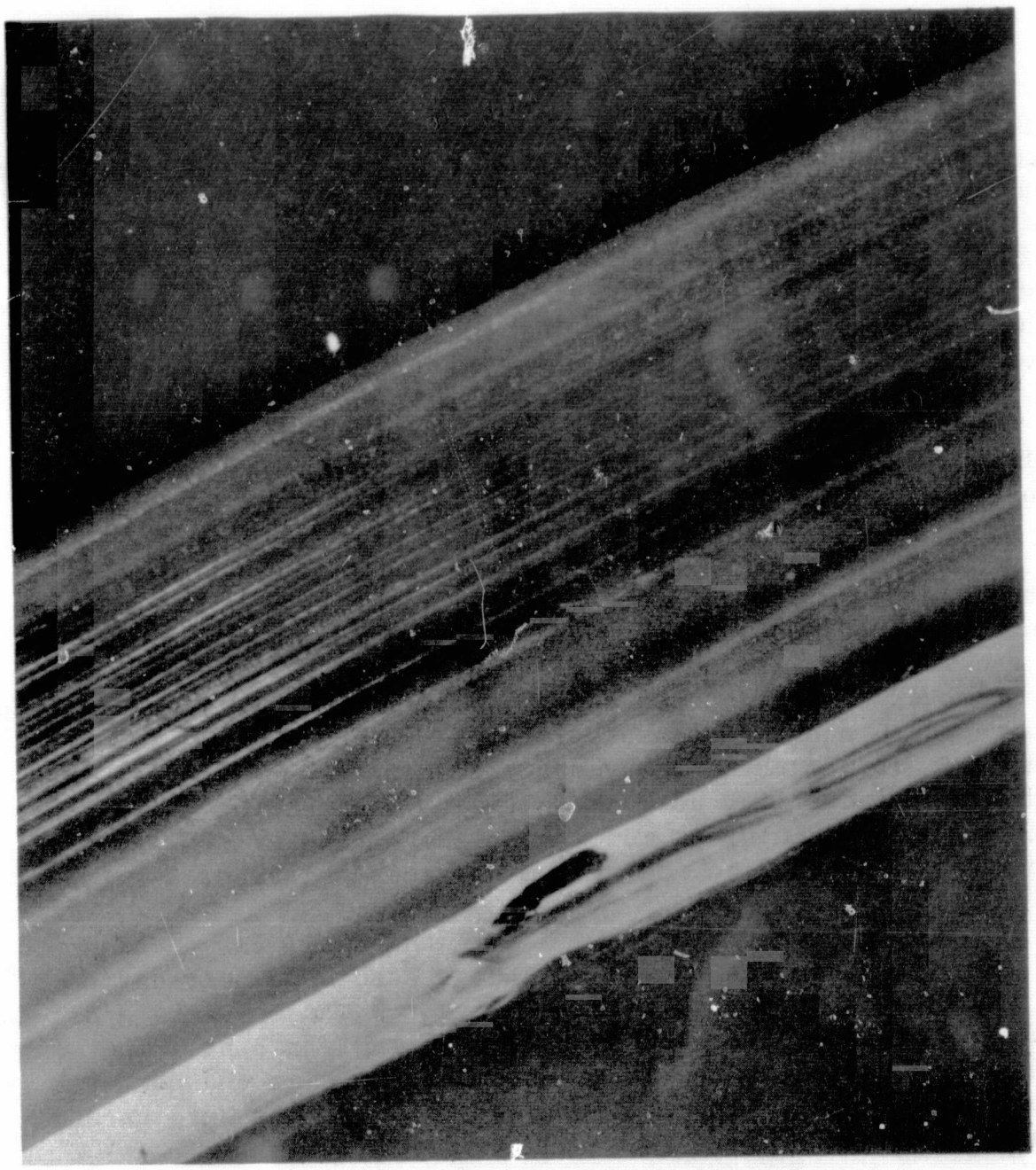

Fig. V-18 Oxidizer Diaphragm Failure Area

A conference was held with the diaphragm vendor, Dilectrix Corporation of Farmingdale, N. Y. During that conference it was suggested that the remaining diaphragm be heated in the upper dome area of the diaphragm to induce a uniform stretch into the tank hemisphere. The vendor's experience with this type of a diaphragm configuration indicated that a stretch up to 4% at room temperature had been obtained. With this knowledge plus the application of heat to the tank wall there was every reason to believe the second diaphragm, S/N 101, would be satisfactory. The diaphragm and tank walls were heated with a hot air gun to approximately 160 to 180°F. The lower half was then assembled and clamped into position. Sufficient force was applied to draw the tank halves to a gap distance of 0.010 in. for welding.

Vacuum was then applied to the upper hemisphere that was at the elevated temperature. A pumping rate of 0.5 in. Hg per minute was obtained and the vacuum successfully reached 29.5 Hg. The tank was then isolated by closing the in-lane valves and the pump removed and the system capped. The tank isolation valve was then reopened and the pressure reading dropped from 29.5 in. to 6 in. Hg. It was then observed for 10 minutes and the readings held steady indicating no leak in the tank either at the girth seal or through diaphragm membrane. The vacuum system was then reinstalled and 29.5 in. Hg vacuum was reestablished.

The tank was then installed in the small vacuum chamber and the girth area was tacked welded to assure no degradation of the seal. When this tack welding operation was complete a differential pressure had been on the diaphragm for 3 hr. The tank was then installed in the large automatic welding chamber with both ends uncapped. The pressure was reduced to a hard vacuum in approximately 1 hr.

Normal weld procedures were then implemented. Weld X-ray were examined carefully and there was no evidence of any weld porosity and the weld was judged successful.

Preliminary leak checks were then attempted before delivery to Wyle Laboratories for formal acceptance tests. The leak check was performed with gaseous nitrogen and an unrestrained flow was developed indicating a severe leak.

When the leak was discovered the tank was filled with alcohol until the level of the leak was determined. Before and after weight determinations showed the leak was in the girth area. The tank was then cut open for examination. The condition of the failure is shown in Fig. V-18 at 10x magnification.

Dimensional Checks - A review of the various pertinent dimensions was made following the failures of the diaphragms. Figure V-15 shows the outline of the diaphragm and the applicable dimensions. The basic tank radius was checked and determined to be 8.250 in. and within the required tolerances. The diaphragms were measured and the results are shown in Table V-3.

Table V-3 Diaphragm Radius

Diaphragm	Radius (in.)		
	Relaxed	Inflated	Required
S/N 101	7.985	8.080	8.080 ± 0.005
S/N 102	7.950	8.078	8.080 ± 0.005

The diaphragm acceptance test plan allows an inflation pressure of 0.4 ± 0.1 psi to provide a stable membrane for the dimensional checks. Table V-3 shows, before the failure, than an inflations pressure of 0.4 psi causes an increase in radius of 0.128 in. reflecting some degradation due to the failure and approaching 2% of the basic dimension.

The following conclusions can be made regarding the diaphragms:

The inflation pressure for reference dimensional checks imposes a stretch of 1.5% on the membrane radius;

Providing an additional stretch from this reference of 2% led to the failure of both diaphragms;

While the application of heat allowed diaphragm S/N 101 to stretch, continued application of the driving pressure force after removal of the heat caused the diaphragm to rupture;

A design approach that provides line-to-line contact of the diaphragm and the tank wall within the 1.5% stretch of the 0.4 psi inflation pressure should be adopted.

The following corrective action was initiated. Two new diaphragms were ordered incorporating the design approach described above. Final tank dimensional adjustments were made to accomodate the affect of cutting the tanks apart. The diaphragms were resized so that a line-to-line contact with the tank wall was achieved. The final dimension was 8.20 in. in radius, which resulted in no more than 1% stretch of the diaphragm from the relaxed condition.

As a result of the diaphragm leakage and subsequent opening of the tank some material was lost. To build identical diaphragms it was necessary to reduce the height of both propellant tanks as dictated by the module tank drawing LAB 6002514-89. The tanks had to be remachined in preparation for rewelding. The -89 tank was reduced 0.155 in. and the tank LAB 6002514-109 was reduced 0.150 in. A fit check of the diaphragms in each tank was satisfactory. The diaphragms in the relaxed condition barely touched the hemispherical wall, which meant the line-to-line contact would be established with less than a 1% stretch.

New fixturing was provided for the tank assembly at this time. The fixtures were heavy duty rings with through bolts that provided assembly of the tanks with the necessary preload to seat the diaphragm ring seal. It also made it possible to make seal leak checks before welding so that repairs could be made if necessary without the expense of cutting the welded tanks apart. Preliminary checks were made before welding with GN_2 and it was established that no leaks occurred at the test pressure of 1 psig.

Both tanks were welded without incident and acceptance tested. During the acceptance testing there was no external leakage or deformation at the proof pressure of 2050 psig.

Some procedural difficulties were experienced in performing the internal diaphragm leakage tests. When the diaphragm is in a relaxed condition at ambient pressure some air is trapped inside the tank. When the diaphragm is pressurized to 1 psig on the liquid side, the air on the pressurization side must escape. This may be interpreted as leakage by the uninitiated operator. The escape rate gradually lowers to a rate that may be interpreted as a permeation rate. If the rate remains high it can be interpreted as internal leakage. Not enough data are available to establish a convincing permeation rate for the various Teflon laminates. Calculations for the geometry of this diaphragm would indicate a helium permeation rate of 15 ml/hr. This assumes a rate of 0.17 ml/in.^{2}-hr-psi-mil obtained from private conversations with Howard Stanford of JPL. This rate was experimental data for FEP Teflon from DuPont. The module tank (-89) leakage was recorded as 5 bubbles of helium in 42 seconds when exposed to the established acceptance test. The tank was returned to the vendor (Pressure System Incorporated) (PSI) where the diaphragm was cycled to an internal pressure of 100 psi and retested with nitrogen. The final rate was 0.165 ml/hr. This compares to a calculated permeation rate for nitrogen of 0.15 ml/hr from the same reference noted above. The component tank (-109) leakage was recorded as 0.6 ml/min before proof test and 1.3 ml/min after proof

test. This compared to 3.8 ml/min on the initial delivery in 1967. Therefore the same acceptance rationale prevails. The leakage rate is not detrimental to the firing time and the alternatives were too costly to consider. Therefore both tanks were accepted.

2. Fuel Tank

a. Description of Changes - During the earlier component testing performed as part of the original work statement the fuel tank screen trap did not perform properly under -1 g conditions. Single phase outflow of propellant was not established. In every attempt a severe entrainment of bubbles was experienced.

A failure analysis was initiated to investigate two potential causes for the two-phase flow. Consideration was given to leakage tests and dimensional checks and a trap was installed in a transparent test fixture to visually observe the flow phenomena. Both the leakage and dimensional checks as well as the visual observations were helpful in establishing the cause of two-phase flow.

The bubbles were observed flowing through the attachment area between the titanium ring and the steel body. The joint is formed by a ring of rivets that were leaktight through the joint; however, the leak path was between the surfaces shown by the arrow in Fig. V-19. This series of tests clearly showed bubbles emerging from the ring area resulting in a well established two-phase flow. Sealing the joint with putty resulted in the desired single-phase flow.

Earlier investigations of the dimensional configurations, leakage, and computed pressure drops were also fruitful. Leak check data revealed the trap in the component propellant tank broke down at 1.5 in. H_2O. This leakage was through the rivet holes at the bottom of the trap. Careful examination and measurement of the as-built condition revealed that the clearances between the shoulder of the trap and the tank wall would develop a pressure drop in excess of 1.5 in. H_2O at system rated flow. Figure V-20 shows the trap installation into the propellant tank.

A parallel effort was started that would lead to the proper design changes for the trap and rebuild schedule for the fuel tank assembly. The trap was modified to eliminate the rivets at the bottom of the trap and provide a greater flow clearance at the shoulder of the trap. This reduced the flow pressure drop in this area to 0.127 in. H_2O and further eliminated the potential leak path through the rivet holes.

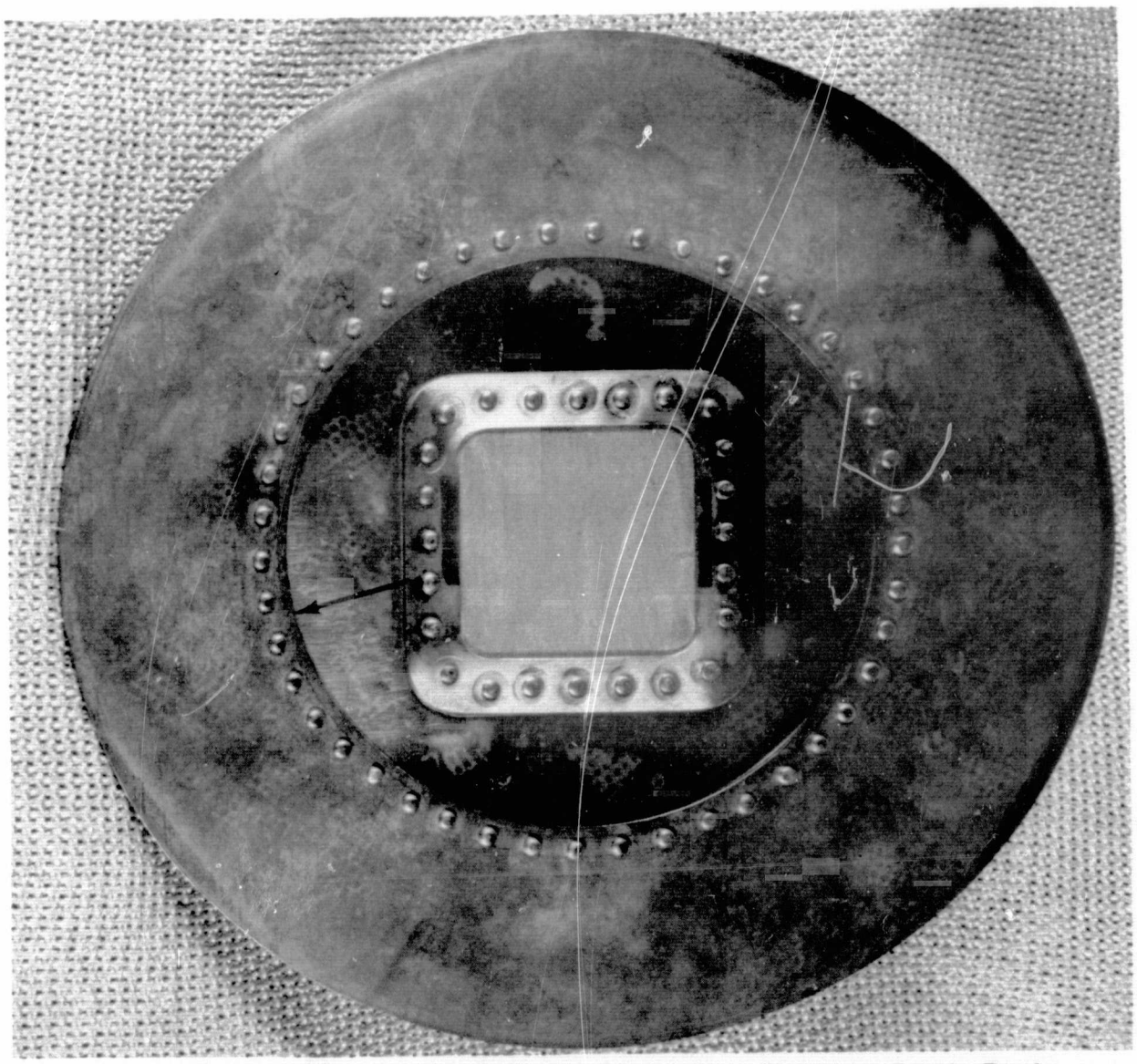

Fig. V-19 Typical Trap Assembly Showing Leak Path

While the new trap was being built, a search was initiated to find a compatible method of sealing the titanium to stainless steel surface at the rivet diameter. First, metallic type sealants, such as soft solders and brazes, were considered. The low temperature solders and brazes, up to 1200°F, were discarded because the fluxes necessary to wet the titanium might cause the fuel to decompose. One high temperature braze of gold-nickel could be accomplished, but this would require a brazing temperature of approximately 1800°F. This high a temperature might cause the rivets to loosen or the screen to degrade, a risk that was not attractive. Therefore the metallic sealants were discarded from further consideration, and attention was focused on the nonmetallic sealants. The nonmetallic sealants had to be tested to prove sealing ability and compatibility with the fuel (MMH) at the sterilizing temperature of 135°C.

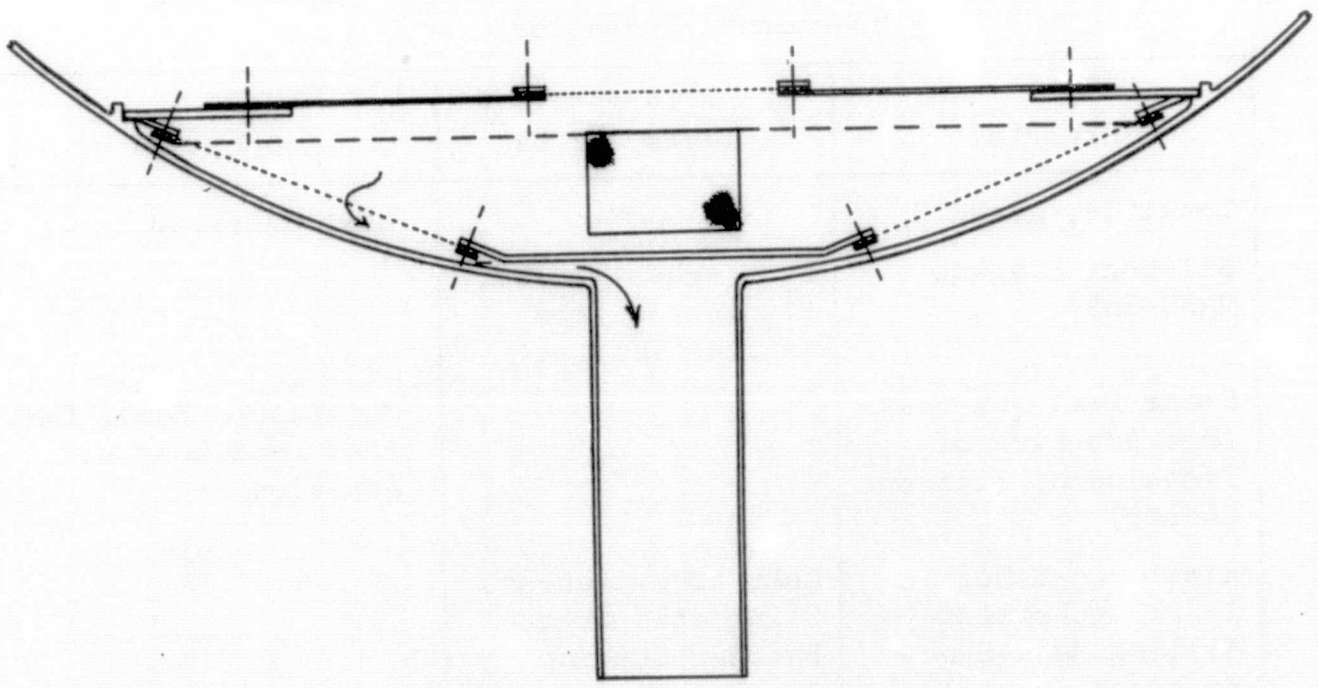

Fig. V-20 Fuel Tank Trap Installation

A series of candiate sealants were tested for qualification. The tests were:

Initial tests at room temperature in monomethyl hydrazine;

Sample joints were made to test for leak tightness before and after fuel exposure;

Exposure of the sealed joints in fuel at 135°C for 114 hr.

Table V-4 presents the candidate materials and the results of the testing.

Table V-4 Results of Nonmetallic Seal Exposure in Monomethyl Hydrazine

Material	Room Temperature Tests, 72 hr	135°C, 114 hr
Locktile, grade H	OK	Lost Adhesion
Silicone Sealant MMSK-138	Lost Adhesiveness, Eliminated from Further Testing	--
Clear Seal (GE Flexible Adhesive of Translucent Silicone Rubber)	OK	Maintained Seal, Excess Bead Lost All Adhesion
Elasto-Coat No. 1-2020 (Chemical Milling Mask Manufactured by Organo-Cerams Inc.)	Lost Adhesiveness, Eliminated from Further Testing	--
Water Glass, Sodium Meta-Silicate: NA_2O x SiO_2 (x = 2 - 5)	OK	Good Hard Bead, No Leakage
Dow Corning DC-11 Grease	OK	Dissolved, Seal Destroyed

During the initial testing certain results were clouded because of inadequate cleaning procedures. All subsequent test specimens were cleaned as follows:

Trisodium phosphate bath (20 minutes);

Water rinse;

Immerse in Turco deoxidizing solution (15 minutes);

Water rinse;

Quick dip in nitric acid + HF;

Rinse in demineralized water;

Dry.

The joints made up for the final immersion in hot MMH were fabricated as shown in Fig. V-21. All the sealants were set aside for 24 hr to provide a room temperature cure. All the joints except the DC-11 were leak tested to 3 psi. The joints were then placed in bombs, loaded to a 30% ullage with MMH, sealed, and placed in a bath at 135°C. Pressures rose no higher than 88 psia, which compares favorably to the normal vapor pressure of 63 psia. Pressures were checked at 24 and 48 hr, and finally at the conclusion of the test at 114 hr. No significant change occurred indicating that none of the materials caused decomposition of the fuel.

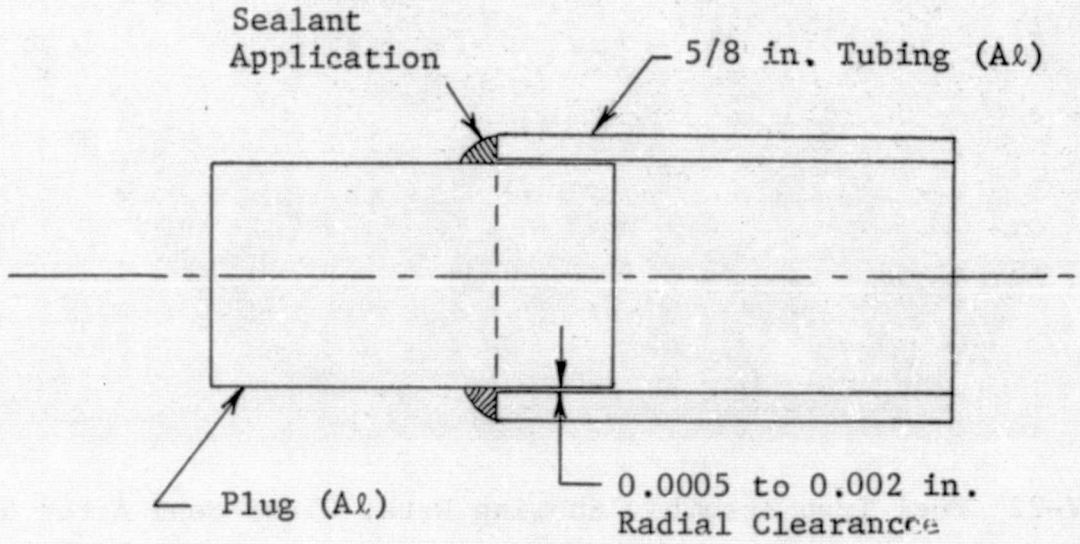

Fig. V-21 Test Joint

To assure that the available trap assembly from the component tank could be properly treated and tested with the water glass, a demonstration was performed. The questionable joint was cleaned with an alkaline solution and water rinsed. Upon air drying methyl ethyl ketone was swabbed around the joint and dried. The water glass was then applied and allowed to dry for 48 hr (see Fig. V-22). The unit was then assembled into the hemisphere and water flow tests proved conclusively the leak between the riveted plates had been stopped as indicated by single-phase liquid flow. These procedures were employed on the trap installed in the modified tank before the final closure weld.

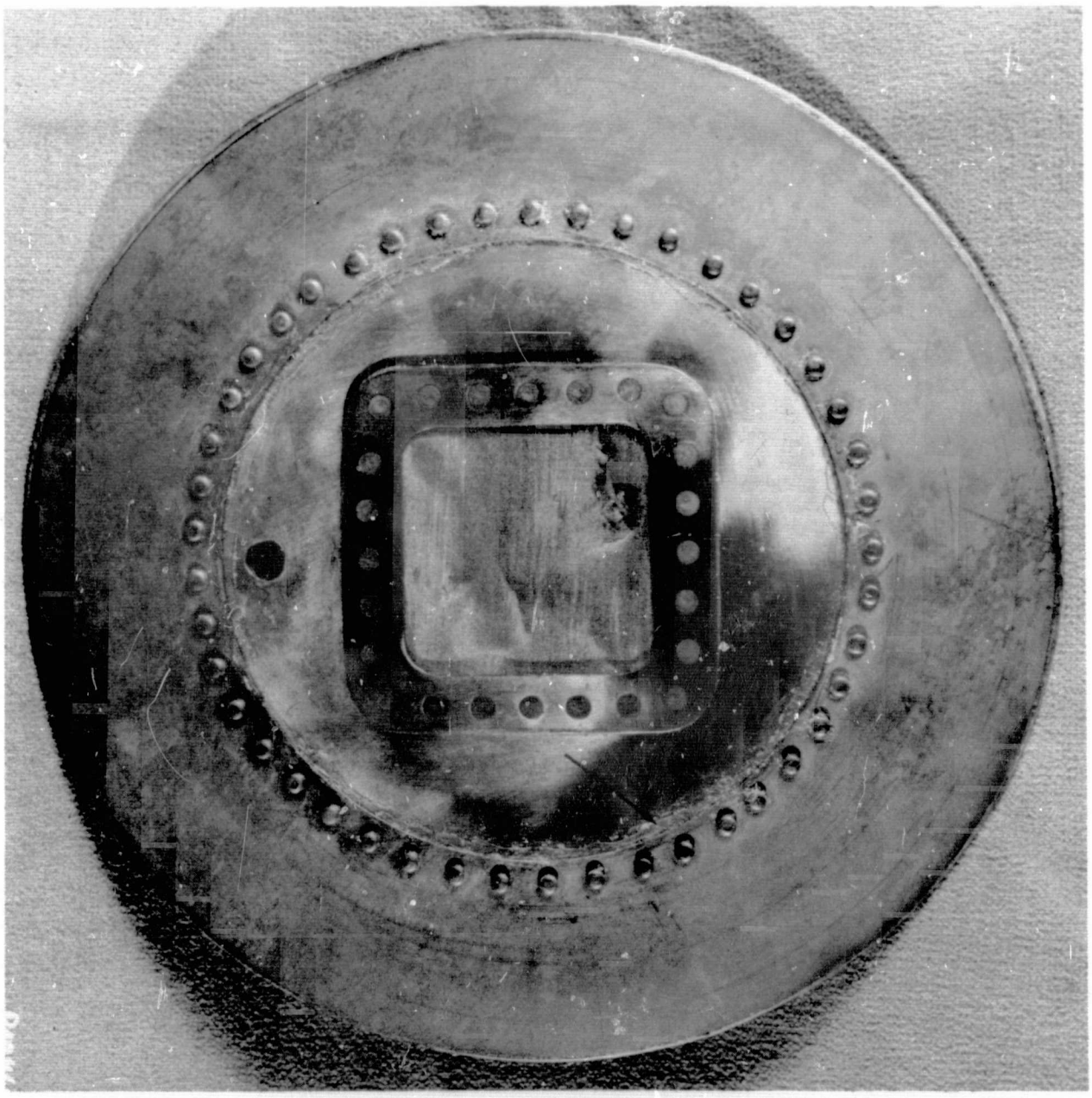

Fig. V-22 Fuel Trap Assembly Showing Water Glass Seal After Test

b. Fabrication - The screen trap selected for modification and installation in the rebuilt module fuel tank was welded in a small evacuated chamber. The completed unit was then passivated in MMH. Repeated attempts to passivate the unit in the fuel were unsuccessful as manifested by continued evolution of gas bubbles signifying decomposition of the MMH. The unit was then immersed in hydrazine in hopes that the hydrazine would reduce the surface catalytic reaction by reducing the surface oxides. The procedure was unsuccessful as noted by continued formation of gas bubbles, though at a somewhat slower rate.

A sophisticated cleaning process was devised to clean the trap unit without destroying the screen cloth. The process included the steps outlined below:

Mask the screens;

Clean outside surface with alkaline solution such as Cee Bee Industrial Cleaner;

Clean outside surface with HNO_3 + HF agent. The cleaning agent was made up of 40% HNO_3/60% H_2O) + 8% HF. Contact with the screens was to be avoided;

Immerse entire unit in a 40% HNO_3 solution;

Rinse in demineralized water.

When the process was implemented, the alkaline cleaner made the surface clean. Application of the HNO_3 + HF foamed considerably. The HNO_3 + HF was repeated four times after which all foaming stopped. The unit was then placed in a bath of hot N_2H_4 at 202°F (local water boiling temperature) for 24 hr. Following the successful verification of passivation, the unit was cleaned in demineralized water followed by an acetone rince and shipped to the vendor for installation in the tank. The completed trap assembly is shown in Fig. V-23 and V-24.

The lower half of the fuel tank was modified by adding more weld material at the point of the trap attachment area. This enabled the trap to be elevated slightly with respect to the tank bottom. When the trap was welded into place in the fuel tank a Martin Marietta engineer applied the water glass to the titanium ring area. The water glass was applied after welding to avoid destroying the bond by the thermal effects of the weld operation.

The fuel tank was then final welded, acceptance tested, and shipped to Martin Marietta Corporation with no further difficulties.

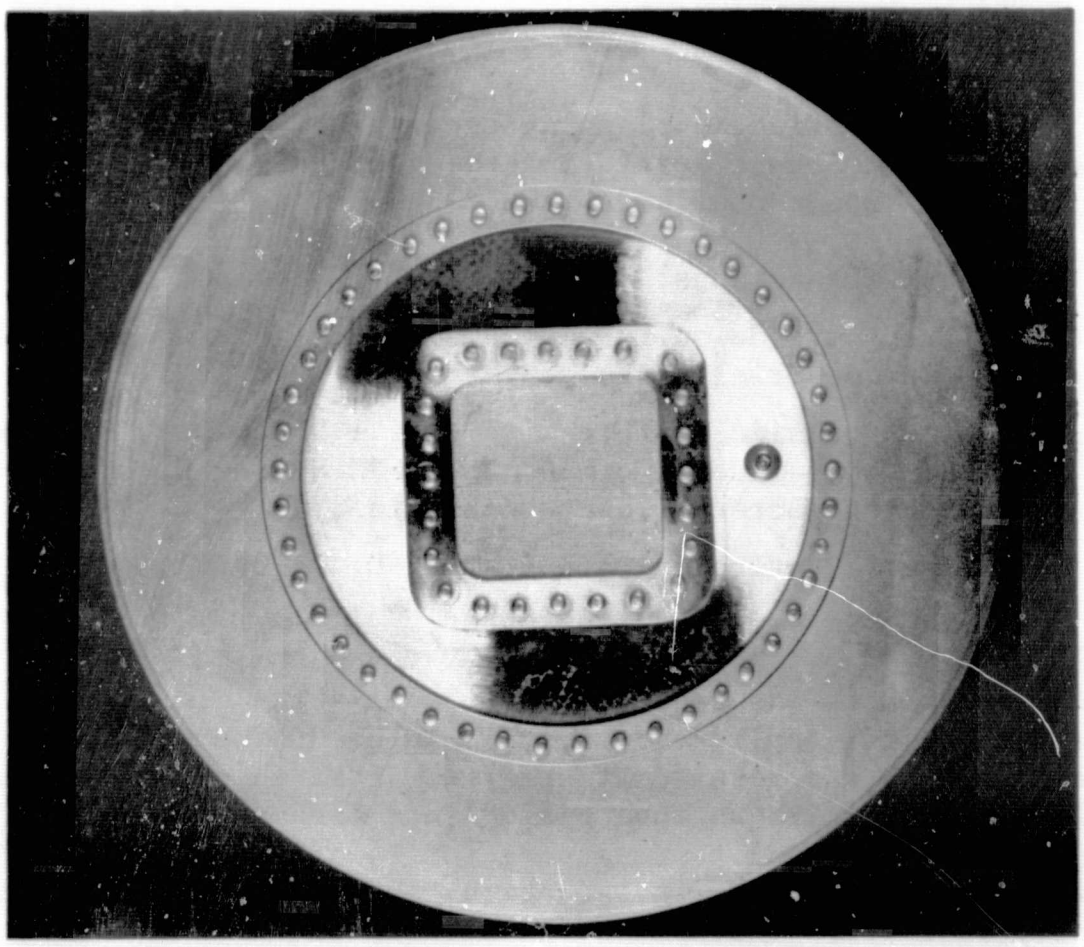

Fig. V-23 Modified Trap Assembly, Top View

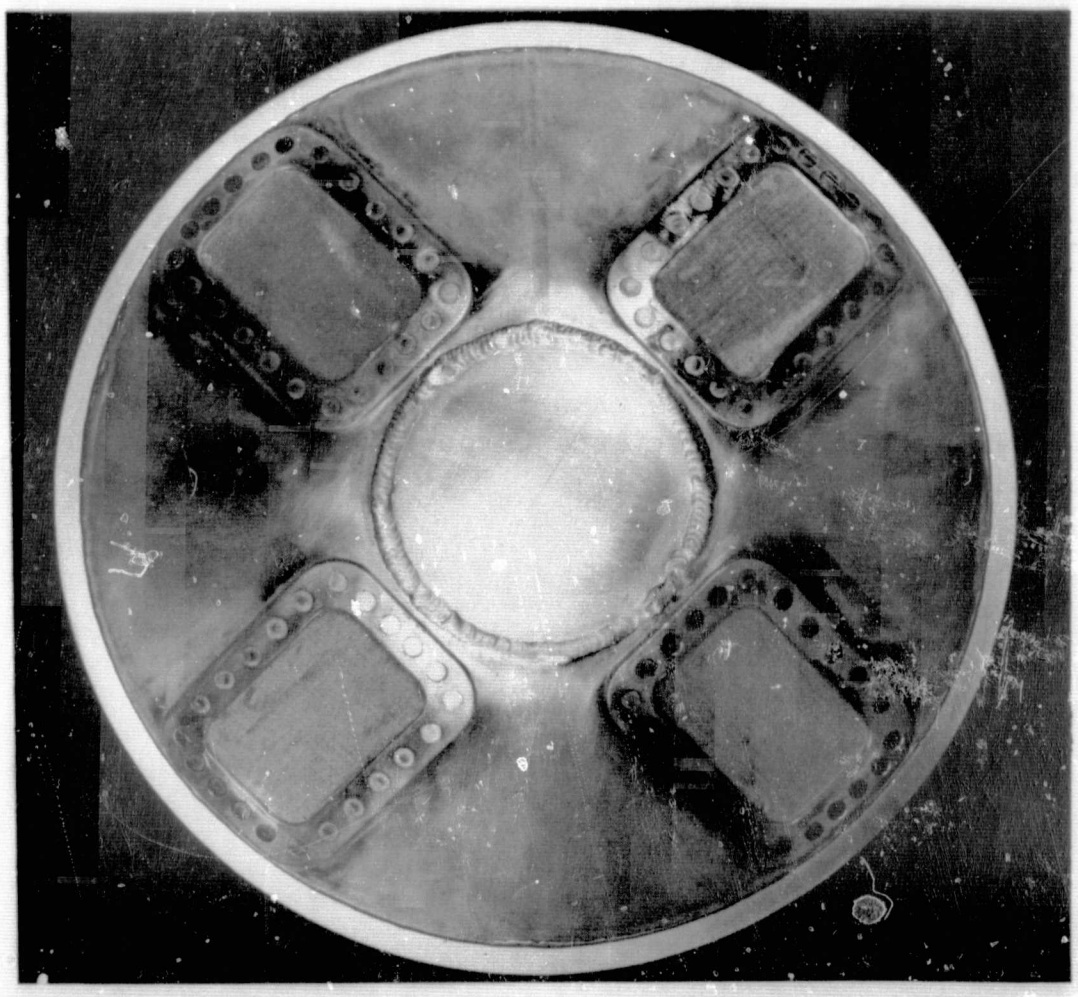

Fig. V-24 Modified Trap Assembly, Bottom View

c. Demonstration Testing - The propellant tank was mounted in the component test fixture for testing according to procedures developed during Phase II of the program. Seventy-four pounds of monomethyl hydrazine were loaded into the tank through successive filters of 5 and 2 microns. The tank was inverted to overfill the trap, eliminating any possible bubble resident below the trap in its normal positive 1 g orientation. Off-loading the tank in a normal 1 g regime to provide the normal fuel load of the tank was accomplished, resulting in a net load of 49 lb. This assured the trap was not submerged when inverted and was indeed retaining the trapped volume of propellant in the -1 g condition. Minus 1 g outflow as completed showing a single phase liquid outflow at a flowrate of 0.13 lb/sec. A fuel volume of 520 cc was discharged as determined by collection in a 1000 ml graduate cylinder.

The computed volume of the trap to the level of the window sectors was 347 cc. The total volume within the tank and outflow system below the trap weld attachment point is 607 cc. Allowing for 5 cu in. of trap volume results in a net volume of 530 cc (Fig. V-25). This would indicated the fuel located outside the trap was swept out in the discharge. The events were recorded on film for future presentations.

The tank was then purged with nitrogen and baked at 150°F for 8 hr. Following this procedure the unit was capped and put into storage until the module was reassembled.

3. Component Inspection and Modification

a. Solenoid - The solenoid valve incorporated in the module was Sterer P/N 35580, S/N 2. After the sterilization exposure and firing, the dielectric strength at 500 vac was 278 μamps. As a result, the No. 27 Formvar wire that does not hold up at 135°C was replaced. The new coil winding incorporates SML magnet wire. The insulation of the bobbin spool and end plates is Micomat wet wound with DC-997 high temperature varnish. All solder attachments, sleeving, and insulation are of high temperature materials. The finished coil was wrapped with a Teflon tape, type P-421. The assembled unit was then baked at 400°F for 1 hr. The valve was acceptance tested and conformed to all requirements. The valve was then returned to the Martin Marietta Corporation for reinstallation in the module.

b. Engine - The Marquardt R4-D engine, P/N X-229663, S/N 0001, was returned to the Marquardt Corporation for inspection and water flow check. To preserve the conditions of the engine for valid continuation of the sterilization program, it was not disassembled. Table V-5 presents representative engine characteristics before and after the sterilization and firing test.

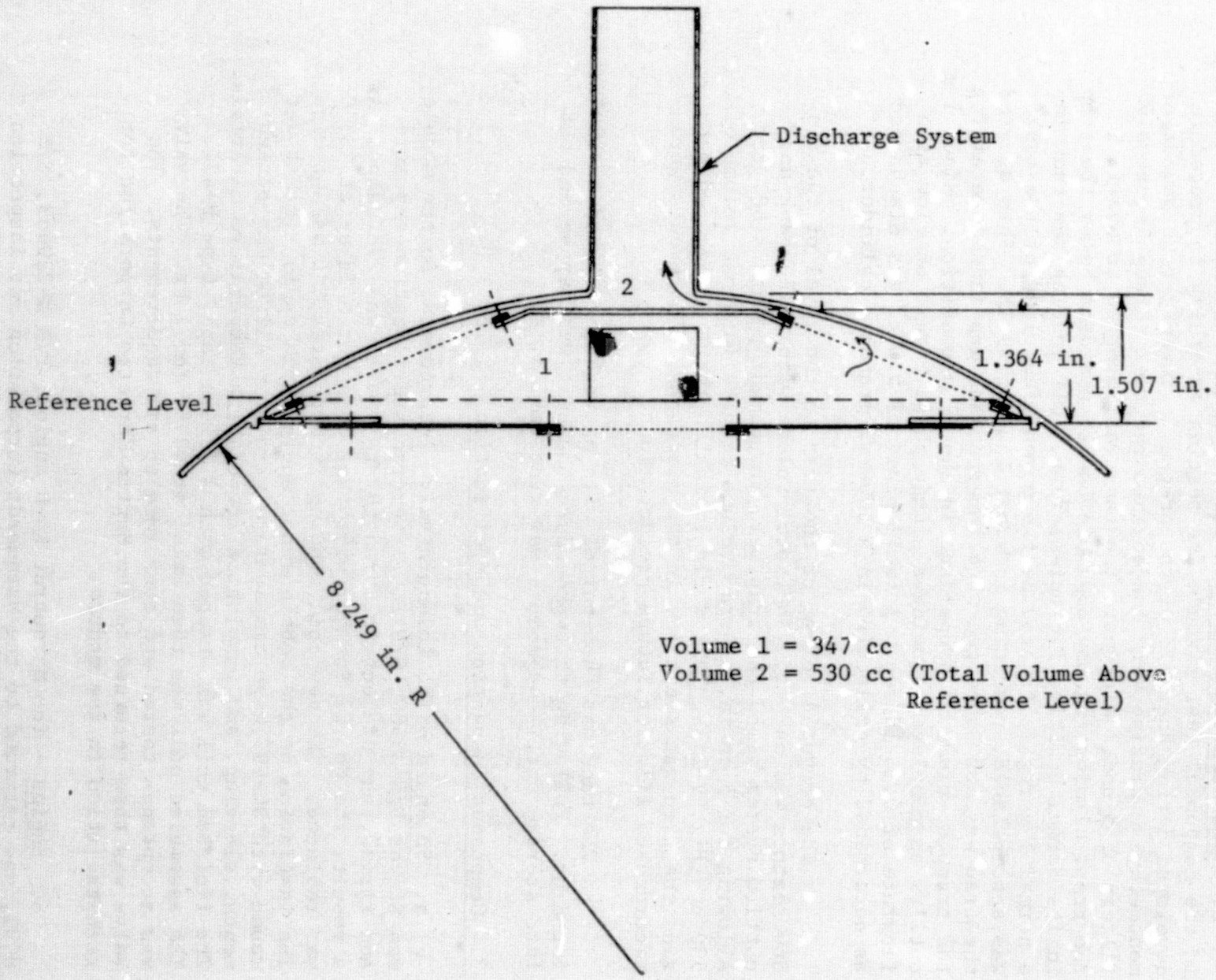

Volume 1 = 347 cc
Volume 2 = 530 cc (Total Volume Above Reference Level)

Fig. V-25 Fuel Tank Trap Volumes

Table V-5 Engine Characteristics

Parameter	Pretest	Posttest
Oxidizer Flow (H_2O/PPH)	552	555
Oxidizer Response (ms)	8.3	8.4
Oxidizer Leakage (scc/hr)	0	0
Fuel Flow (H_2O/PPH)	438	436
Fuel Response (ms)	6.4	6.4
Fuel Leakage (scc/hr)	0.50	0

Table V-5 shows the engine suffered insignificant degradation as a result of the first sterilization program. On this basis, no adjustments were made to the flow control orifices. The engine was returned to Martin Marietta Corporation and reinstalled in the module.

C. SYSTEM ASSEMBLY

When the propellant tanks were received from the vendor the system was reassembled. The assembly activities were performed in the 100 class laminar flow clean room at the Cold Flow Laboratory of the Denver Division.

1. Configuration Changes

Several minor configuration changes were made in the system. None were of a nature to compromise the objectives of the program.

A hand valve was substituted for one of the ordnance valves because a sufficient quantity of JPL-supplied ordnance valves were not available. The ordnance valve in the gaseous nitrogen pressurization system was replaced with a 1/4-in. Republic hand valve. This type of valve had previously been subjected to the sterilization environment as part of a test fixture in the component test phase. Thus, the hermetic seal of each propellant tank was maintained and the hazards of a propellant leak were minimized.

The serrated flange seal on the ordnance valve leaked on several occasions during the previous sterilization exposure. The action taken during the initial build up was to use longer through-bolts at the flange, raise the torque to 40 in.-lb and use backup nuts to relieve the load on the aluminum threads of the valve body. During the program extension the soft aluminum washers used as gaskets in the serrated flange were coated with 1-2 mil of Teflon. Further, during installation of the valves a special tool was used to take up the torque loads as opposed to taking some of the load through the serrated flange joint in question.

A material change was made in the fuel tank drain line. This line in the oxidizer circuit failed during the initial program as a result of thermal stresses set up in the tube. The tube was fabricated with bend radii as small as two times the tube diameter. In the fuel line the tube was changed from 6061-T6 to 300 series stainless steel. This change was a convenience change to allow easier tube bending and flaring. The change was not made on the oxidizer line since the hand valve is open during sterilization and 300 series stainless steel is not compatible with the oxidizer at 275°F.

As a result of the slightly smaller propellant tanks several tubing changes were required during the reassembly to assure a proper fit. This made it necessary to develop new pressurization lines leading from the pressure regulator outlet "cross" to each propellant tank. These tubes were fabricated according to the established drawings, which required the tube to be of 6061-T6 aluminum and 3/8-in. O.D. by 0.035-in. wall thickness.

2. Assembly Verification and Checkout

Several checks were performed to assure proper functioning of the module. The propellant feedline filters were back flushed to assure proper operation. There was never any evidence of contamination present. This was done as a precaution. The pressure system filter was not back flowed. It was welded into the system interfacing directly with the regulator inlet. It was not possible to back flow through the pressurization filter without also back flowing through the regulator. It was decided there was more risk in this procedure than in the improper operation of the filter. Therefore the pressurization filter was not back flowed.

Several of the Vacco hand valves leaked. Four valves were required in the module. Two valves showed no leakage, one was leaking at 2.5 scc/min of GN_2, and one was leaking at 50[illegible] scc/min. The higher leaking valve had been installed in the oxidizer drain line in the closed position.

The stem in the valve was replaced. To replace the entire valve would have required welding and modifying a valve body as described in Part I of the final report. Since the valve seat is hard anodized 1100 aluminum and the stem is 1100 aluminum in the "0" or soft condition it was reasoned that the stem was the only part in poor condition. This rationale was supported by the results of the first sterilization exposure of the component valve, which showed extreme corrosion, and by the results of the materials compatibility program, which showed anodized aluminum as compatible in N_2O_4. The repair of the valve was successful with the new leakage measured at 0.1 scc/min.

The valves were repositioned to put the valves with no leakage in the propellant drain line of either tank, the reworked valve in the oxidizer tank vent position, and the valve with nominal leakage in the fuel tank vent position. In this position the valve is not opened and therefore the risk was minimal. None of the three valves with little or no leakage were disassembled. An objective of the program was to learn as much as possible. If the valves were reworked, degradation added by a second exposure could not be determined.

During checkout after module reassembly, the regulator was found to be inoperative. The action taken was to cycle the inlet pressure between zero and 350 psig rapidly while tapping on the regulator diaphragm housing lightly with a plastic mallet. This action did cause the regulator to begin operation. The initial leakage of the unit on a 0.5 cu ft ullage resulted in a pressure rise rate of 68 psi/min. Repeated cycling improved the operation of the regulator so that the final leakage rate was 26.4 scc/hr. This compares to a specification value of 10 scc/hr and 14.5 scc/hr at the initiation of sterilization on the initial buildup. After sterilization and before the first firing the regulator leakage was zero.

The lack of operation of the regulator was a significant program result. The 16-month shelf storage of the regulator is the same order of magnitude as a mission to the near planets. Mission success would depend on regulator operation.

Each component was exercised to obtain the appropriate performance data for a baseline before sterilization. These data are presented and compared to past sterilization data in a later section of the report.

3. Propellant Loading

New propellant loads were established for this firing because the modified propellant tanks were slightly smaller than the original design. The original tanks had a volume of 2350 cu in.

The fuel tank volume was reduced by the material lost in cutting the tank in two pieces following the initial firing. The oxidizer tank was redesigned to put the diaphragm on the centerline and reworked to accomodate the separation following the diaphragm rupture during assembly. The resulting tank volumes then were:

Fuel, 2217 cu in.;

Oxidizer, 1937 cu in.

The maximum loadable quantities based on propellant densities at 135°C were as follows:

	Density (lb/cu ft)	Maximum Loadable (lb)
Fuel	47.95	61.4
Oxidizer	64.30	70.5

The propellant loading inventory for each tank established on the basis of a 290-sec run is given in Table V-6.

Table V-6 Propellant Loading Inventory

	Fuel	Oxidizer
Flow Rate (lb/min)	8.69	13.91
Usable, 290 sec (lb)	42.00	67.10
Decomposition 4%, 0.5% (lb)	1.68	0.35
Propellant sample 60 cc (lb)	0.12	0.20
Trapped in feedline (lb)	0.06	0.30
Loading uncertainty (lb)	0.50	0.50
Outage, 2% (lb)	0.84	1.39
Fuel bias (lb)	1.26	--
Total	46.46	69.84

Actually loaded aboard the module were 51 lb of fuel and 70 lb of oxidizer.

The planned run time was 280 sec based on earlier precedent set for the first firing during the readiness review. The run time was selected on the basis that the system was not fully qualified and only limited performance history was available. The placement of the diaphragm on the equator of the oxidizer tank meant the diaphragm could be cycled through from top to bottom. Previously the diaphragm was 0.8 in. above the equator, resulting in 10.60 lb of oxidizer trapped in the tank. This explains why the tank volume could be reduced 413 cu in. and still achieve the same run duration as obtained in the initial module assembly.

D. SYSTEM STERILIZATION EXPOSURE

The module sterilization exposure began on April 14 and was completed on April 23, 1969. The exposure consisted of three 30-hr cycles at 135°C or 275°F. Each cycle included a 6-hr heating phase at 19°C/hr and a 6-hr cooling phase at the same rate for a total cycle time of 42 hr.

Cycle 2 was extended and penalized because of an inadvertant shutdown resulting from an abnormality in the facility controls. The system accumulated 38 hr at 135°C as verified by fuel tank total pressure.

Table V-7 presents the typical values of module and chamber parameters of importance.

Table V-7 Sterilization Data

Cycle	Chamber Temperature (°F)	Oxidizer Tank Pressure (psia)	Fuel Tank Pressure (psia)
1	274	820	85
2	275	810	83
3	274	830	83

The values in Table V-7 agree with the experience of the previous sterilization exposures. The fuel pressure indicates some decomposition took place, but no more than previously. The expected vapor pressure of MMH at 135°C is 63 psia. The data indicate the decomposition discontinued during the initial cycle.

The spread in the oxidizer pressure equals 20 psi. This spread is not unreasonable when it is realized that a 1500-psi gage was used for the recordings. A spread of 20 psi represents a 1 1/3% spread or $\pm$2/3%.

E. SYSTEM FIRING READINESS

Before the second firing attempt a readiness review was conducted. The propellant sample assay results were reviewed, the component functional characteristics were verified, and the operational procedures were reviewed.

1. Propellant Samples

During the prefiring readiness review period the fuel tank trap from the component unit was examined. The inspection revealed the water-glass sealant was sloughing off the unit after a shelf storage of 9 months. The water glass had been applied to the top of the trap to seal the faying surfaces so that propellant outflow could be demonstrated in a -1 g regime. Earlier compatibility tests with hot fuel demonstrated compatibility, but the requirement for a passivation procedure with a 75% water/25% fuel mixture was overlooked. Since the water glass was installed in the module tank after the trap was welded in the tank, the possibility of water glass particles entering the propellant feed system and being trapped on the 5μ filter upstream of the engine was of primary concern.

A propellant sample withdrawn from the fuel tank after the second sterilization cycle did show a considerable contamination level. On the basis of this result a test was conducted to determine if the water glass that was in the hardened state was soluble in water. The solubility test of the water glass in the 75% water/25% fuel fixture gave positive results. An additional sample was withdrawn from the module after the final sterilization cycle for analysis. The results of this and all of the propellant sampling is presented in Table V-8. The analysis of the final sample indicates the fuel was suitable for firing.

This may be explained by the sequence by which the water glass was applied to the trap. As noted above, the water glass was applied to the top surface of the trap only after the trap was welded into the fuel tank. In effect the propellant must pass through the two screens of the trap rated at 30μ and then pass through a 5μ filter before entering the engine. On the basis of the results in Table V-8 and the rationale above, it was concluded the propellant condition was satisfactory for the engine firing.

Table V-8 Propellant Sampling Results

Sample Source	Sample Results	
	Oxidizer	Fuel
Facility Supply (before loading)	N_2O_4, 98.64% NO, 0.59% H_2O, 0.11%	MMH, 98.12% H_2O & Misc, 1.88% (Barrel S/N H5048)
Module Loading System (Presterilization)	N_2O_4, 99.95% NO, Not Reported H_2O, 0.01%	MMH, 99.03% H_2O & Misc, 0.97%
Module Fuel Tank after 2nd Sterilization Cycle		Particle Size (μ) / No. 50-250 / 85 250-600 / 4 600-1000 / 7 >1000 / 2
Module Tanks After Final (3rd) Sterilization Cycle	N_2O_4, 99.04% NO, 0.48% H_2O, 0.02%	MMH, 98.90% H_2O & Misc, 1.10% Note: One 300μ particle of resinous appearance; two smaller silicious particles (approx 30 to 50μ).

2. Component Functional Verification

After the second series of sterilization cycles the module was removed from the chamber and installed in the firing test stand. The engine thrust chamber valves and the regulator performance were paramount to the module operation. The performance of these and the solenoid valve were checked in accordance with established procedures. The results of these tests and of those conducted before the sterilization are presented in Table V-9. The continuous data for the regulator and thrust chamber valves are valid. For the solenoid valve rebuilt to overcome the coil wire insulation breakdown, the shelf life experience is not valid. The valve was rebuilt and returned to the module in September 1968. It was then installed on the module and not actuated until April 1969. No difficulty was experienced with the valve.

Table V-9 Component Performance History

Component	October 1967, Initial Condition	January 1968, Poststerilization Exposure, 6 - ETO, 6 72-hr Cycles	April 1969, Dormant Storage	April 1969, Poststerilization Exposure, 3 30-hr Cycles
Thrust Chamber Valves				
Oxidizer Valve				
Opening Response, max/min (sec)	0.0092/0.0089	0.0098/0.0095	0.0099/0.0097	0.0091/0.0088
Closing Response, max/min (sec)	0.0062/0.0060	0.0068/0.0061	0.0077/0.0066	0.0081/0.0075
Leakage - External (bubbles GN_2)	0	0	0	0
Internal (cc GN_2/hr)	0	0	0	0
Fuel Valve				
Opening Response, max/min (sec)	0.0073/0.0070	0.0078/0.0068	0.0080/0.0077	0.0074/0.0071
Closing Response, max/min (sec)	0.0070/0.0062	0.0078/0.0075	0.0085/0.0074	0.0080/0.0077
Leakage at 250 psig:				
External (bubbles GN_2)	0	0	0	0
Internal (cc GN_2/hr)	12	0	0	0
GN_2 Loading Solenoid Valve* (1) MMC P/N LAB 6002516-001 Sterer P/N 35580				
Leakage, External (scc/sec helium)	0	0	0	0
Dielectric Strength (μ amp at 500 VAC)	6	278	104	114
Regulator MMC P/N LAB 6002515-009 Sterer P/N 35540 S/N 2				
Internal Leakage (scc/hr GN_2)	14.5	0	26.4	24.4
External Leakage (bubbles GN_2)	0	0	0	0
Regulation:				
Inlet Pressure, Initial (psig)	1498	1528	1550	1530
Inlet Pressure, Final (psig)	350	350	350	350
Average Flow Rate, GN_2 (lb/sec)	0.015	0.014	0.015	0.014
Outlet Pressure Var, max/min (psig)	250/247	248/244	244/240	246/242
Hysteresis:				
Initial Outlet Lockup Pressure (psig)	263	259	259	257.5
Outlet Pressure Range (psig)	250/247	258/252	250.5/259	251/258.5
Response:				
Inlet Pressure, Average (psig)	1520	1517	1420	1415
Outlet Pressure, Lockup (psig)	261	257	258.5	258.5
Overshoot (psig)	0	0	0	0

*The solenoid coil was rewound with high temperature materials after first sterilization and firing.

The engine thrust chamber valves show some scatter in the response time figures but the proper lead time of fuel leading the oxidizer valve was maintained in every case. In general the Marquardt engine propellant valves were trouble free, and therefore very high in reliability.

The regulator, after smooth operation was established, achieved performance within specification limits on every item except leakage. The internal leakage of the system did degrade and was erratic over the time period under discussion. The regulator was welded into the module and therefore was not given any special care. The system was opened to remove the propellant tanks and then reassembled under the clean conditions established for this program.

As a result of the values shown in Table V-9, it was concluded that the components were performing adequately and a firing could be conducted with confidence.

3. Procedures

All necessary procedures were updated to reflect the current configuration and sterilization exposure. The manual valve incorporated in the system in place of an ordnance valve between the pressurant tank and regulator inlet required procedural changes to open the valve before clearing the personnel from the firing stand.

The contract requirement for three 30-hr dry heat sterilizations also required new procedures that were generated and approved.

F. SYSTEM FIRING

Following the three 30-hr dry heat sterilization exposures and system functional checkout the system was prepared for a firing on April 29, 1969. This firing was aborted when the pressurant storage pressure bled down to zero following actuation of the ordnance valves.

Following an investigation of the condition of the module, corrective action was agreed to with the contract technical monitor and implemented for a later firing attempt. The second firing attempt on May 2, 1969 was successful.

Each of the firings are described in the paragraphs below.

1. First Firing Attempt

The schematic of the module configuration is shown in Fig. V-26. The procedure was followed normally through opening of the hand valve and pressure regulator lockup. Lockup pressure was 262 psig. After a short delay to correct a power problem on the firing stand, the pressures of the storage sphere and regulator outlet pressure were as follows:

$$P_{nt} = 1600 \text{ psig;}$$

$$P_{ro} = 269 \text{ psig.}$$

The next step in the procedure was to actuate all of the ordnance valves to drop propellants to the engine and pressurize the propellant tanks. When this step was implemented the pressure in the gas storage sphere bled down to zero. A review of the data showed the propellant tank pressure only reached pressures of

$$P_{ot} = 119 \text{ psig at } 27 \text{ sec;}$$

$$P_{ft} = 117 \text{ psig at } 26 \text{ sec.}$$

The rise rate of the propellant pressures was very slow. A technician near the test stand was able to detect gas escaping from the system. When the propellant tank pressures bled down to zero it was decided to isolate the propellant tanks by closing the fuel tank isolation valves located on top and bottom of the tank so the hypergolic vapors could not react further.

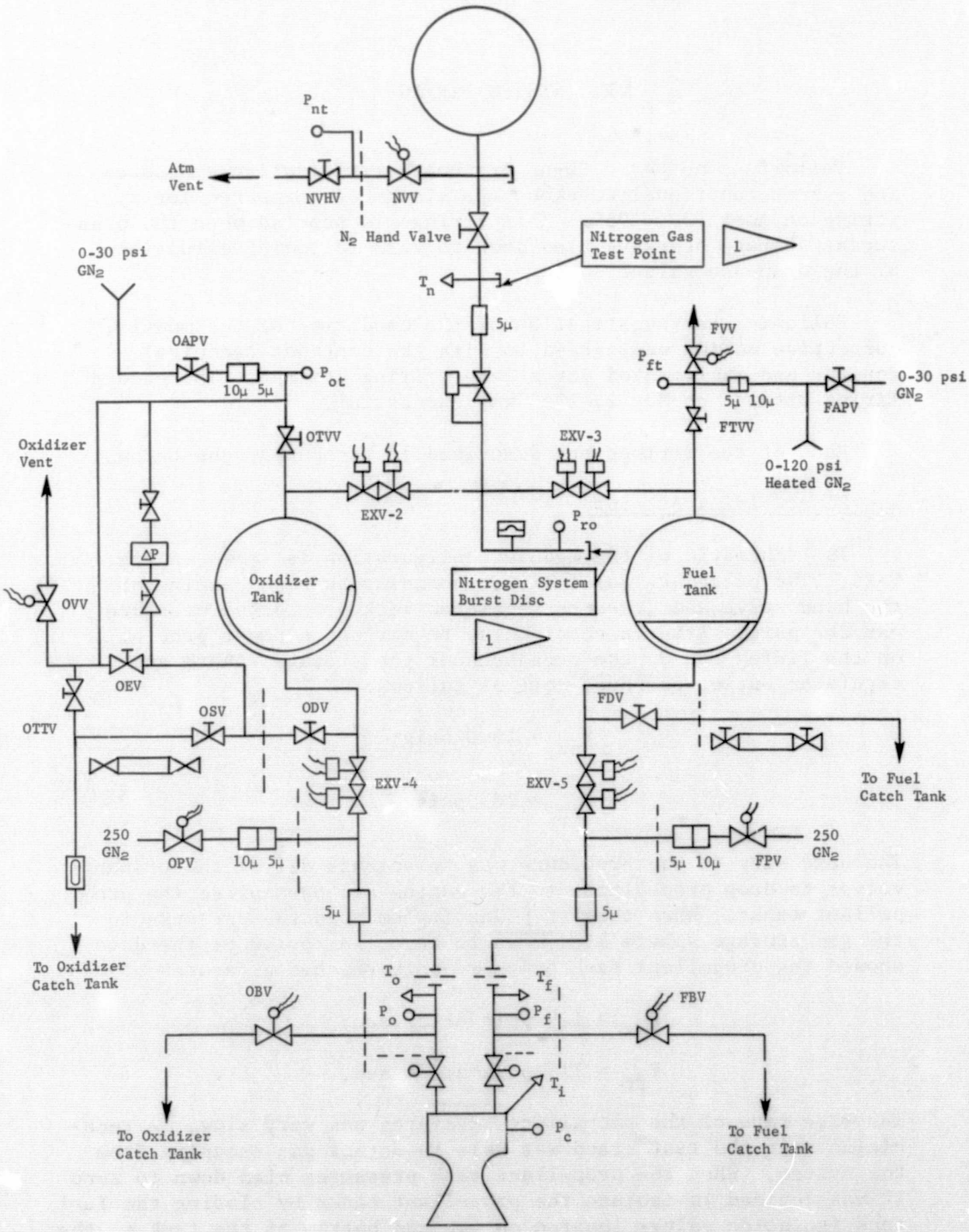

Fig. V-26 Firing Test Schematic

Investigation and examination of the module revealed the pressurization line just upstream of the ordnance valve, EXV-3, had a sizable hole in it. Figures V-27 and V-28 show a close up of this line and failure.

A careful review of the condition of the module revealed no other abnormal conditions or functions. Since the objectives of the program were concerned with the module performance using sterilized propellants it was decided, with the concurrence of the contract technical monitor, to alter the system plumbing and refire the module without off loading the propellants.

2. Cause of Failure

A close examination of the data traces revealed: (1) the regulator pressure and pressurant tank pressure were constant before the ordnance valve actuation; (2) the propellant tank pressure rise rate was approximately one-half the value of the initial firing; and (3) the rise rate was lower from the very initiation of pressurization. The tank top traces are shown in Fig. V-29.

The above circumstances directed our attention to the ordnance valve to find the cause of failure.

The ordnance valve from position EXV-3 was removed from the system when it was available and sectioned for complete examination. Figure V-30 shows the valve after it was sectioned. From the figure the cause of failure was quite apparent. The portion of the valve to the left is the normally closed half that does not contain a guillotine or plunger as it would if it had been assembled properly.

The failure sequence was initiated at the ignition of the ordnance squib (not shown in the figure). The explosive charge burned through the tube plug and entered the plumbing system. The molten aluminum and the burning powder then went both directions from the valve. This would indicate the products entered the fuel tank and the pressurization line. It did not burn through the tube integrally attached to the ordnance valve because the tube wall thickness was approximately 0.100 in. The burning charge then went further upstream into the aluminum tube that was only 0.035 in. in wall thickness. The failure then was at the first curved section of the tube as shown in Fig. V-27 and V-28.

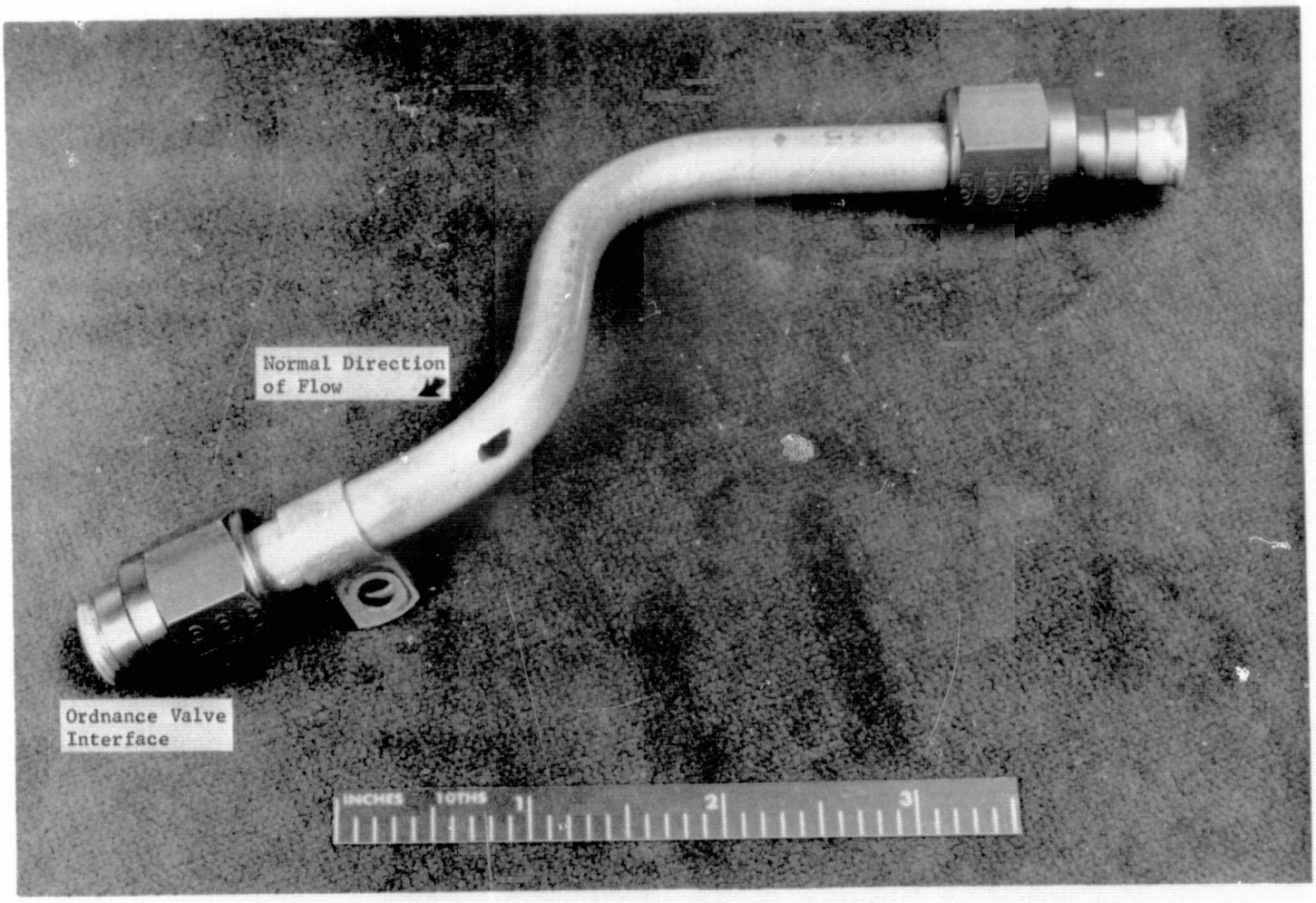

Fig. V-27 Pressurization Tube

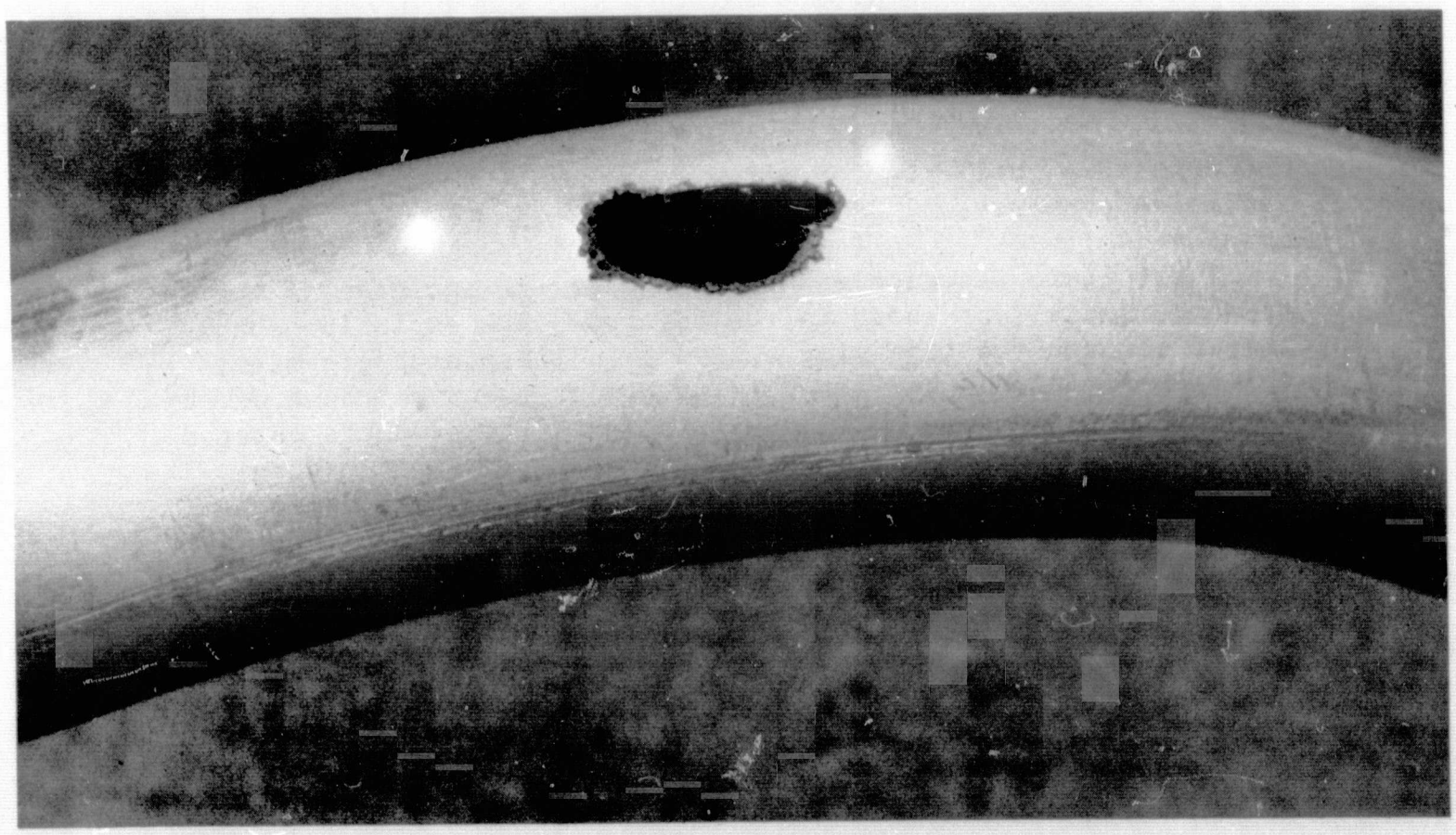

Fig. V-28 Pressurization Tube, Close Up

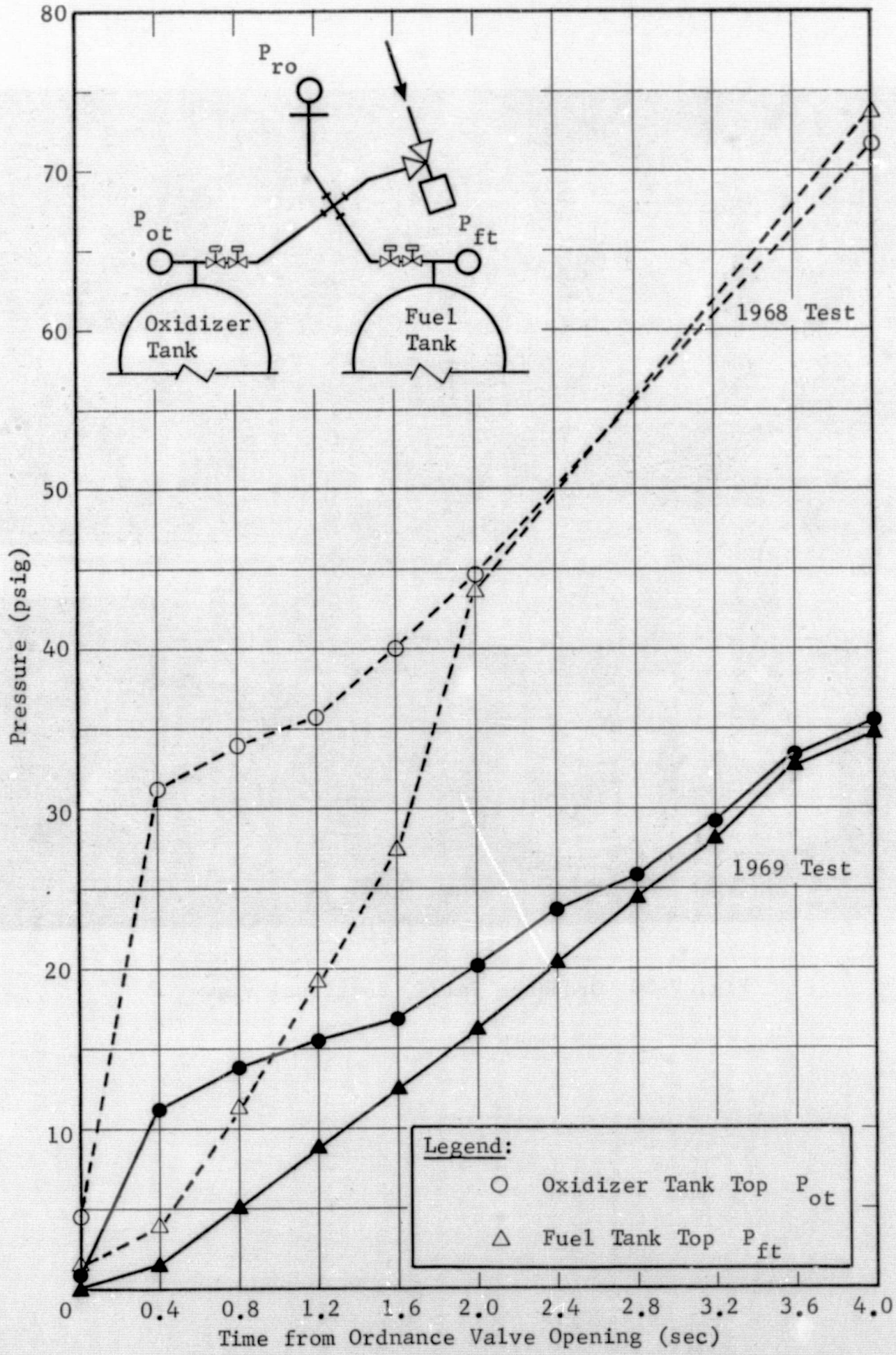

Fig. V-29 Module Pressurization Sequence, Initial Attempt

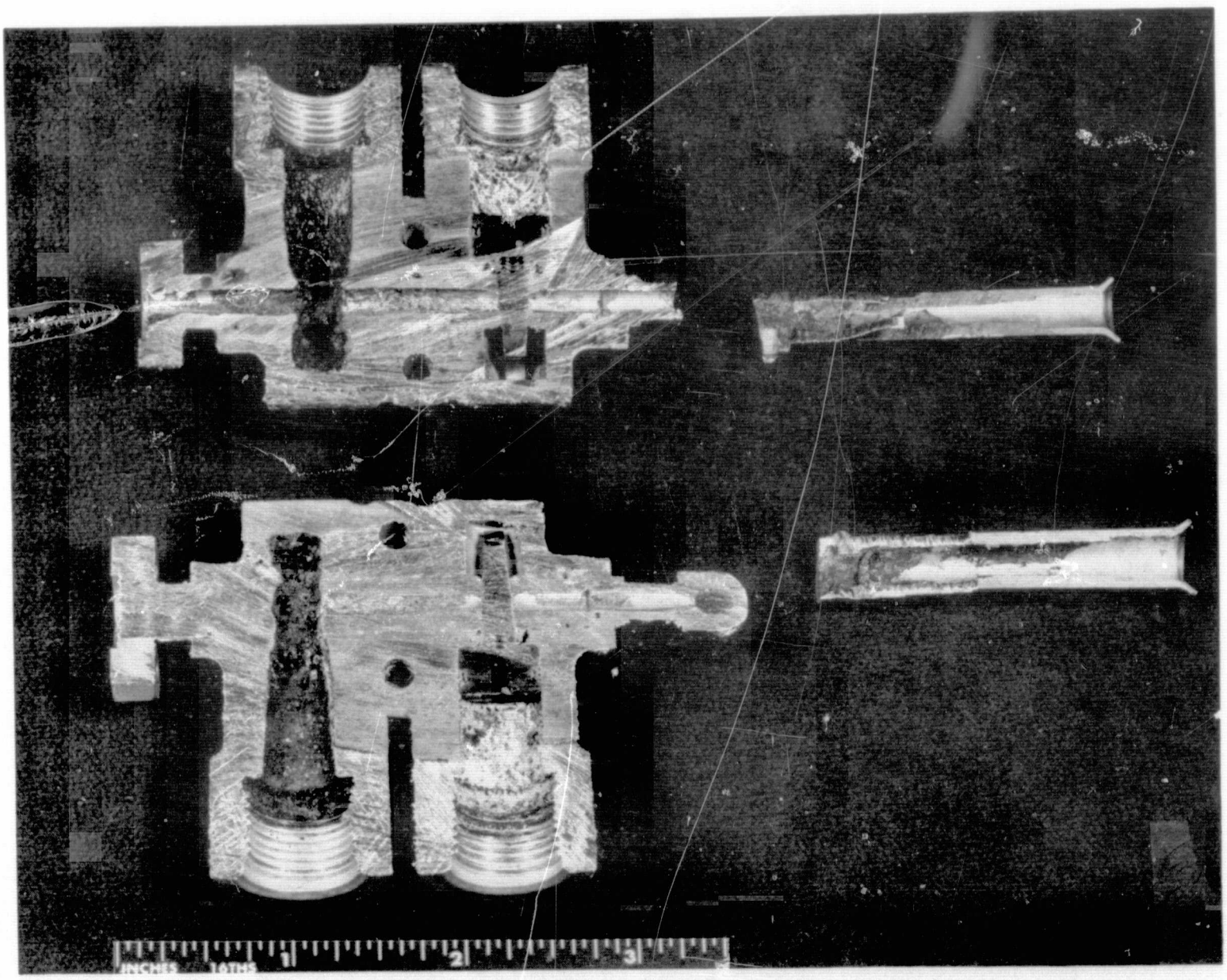

Fig. V-30 Ordnance Valve, Sectional View

3. Recovery Action

The module plumbing was revised to the configuration shown in Figure V-31. This provided a propellant feed system by by-passing the ordnance valves that had been closed in the earlier attempt as a safety precaution.

Before refiring the module the procedures were revised and carefully reviewed to be certain nothing was overlooked in order to quickly refire the module. Calculations were performed to ascertain the engine mixture ratio would still be within acceptable limits.

As a result of the pressure drop calculations it was decided to install 1/2-in. ball valves in the position of FDBV and FPV. This valve size required supporting brackets and longer tube runs so that the valves could be firmly positioned. The larger valves and longer tube runs provided a lower pressure drop than the smaller valve with short coupled tubing runs. The calculated pressure drops and engine mixture ratio are presented in Table V-10.

The longer tube run and unbalanced tube volumes were of some concern. To alleviate any potential problem the fuel line was bled in before the firing to make sure both propellants were hard on the engine thrust chamber valves. This procedure was reviewed with the engine manufacturer. The procedure and calculated engine mixture ratio were both approved by Marquardt.

The module pressurant tank was reloaded with nitrogen to 1590 psia. The new plumbing was leak checked and all the control harness leads were voltage checked end to end to be sure the new functions of valves were properly hooked into the control console.

4. Second Firing Attempt

Following the above checkout activities the engine module was successfully fired for 280 sec on May 2, 1969. Visual observation on the TV monitor and real-time data traces showed proper module operation. The firing operation is shown in Fig. V-32.

Chg A (4/28/69): Add V-2, V-3, FDBV and connecting tubing and change FPV to a 1/2 inch remote ball valve to bypass closed pyrovalves EXV-3 and EXV-5 and to bypass open EXV-2 for control.

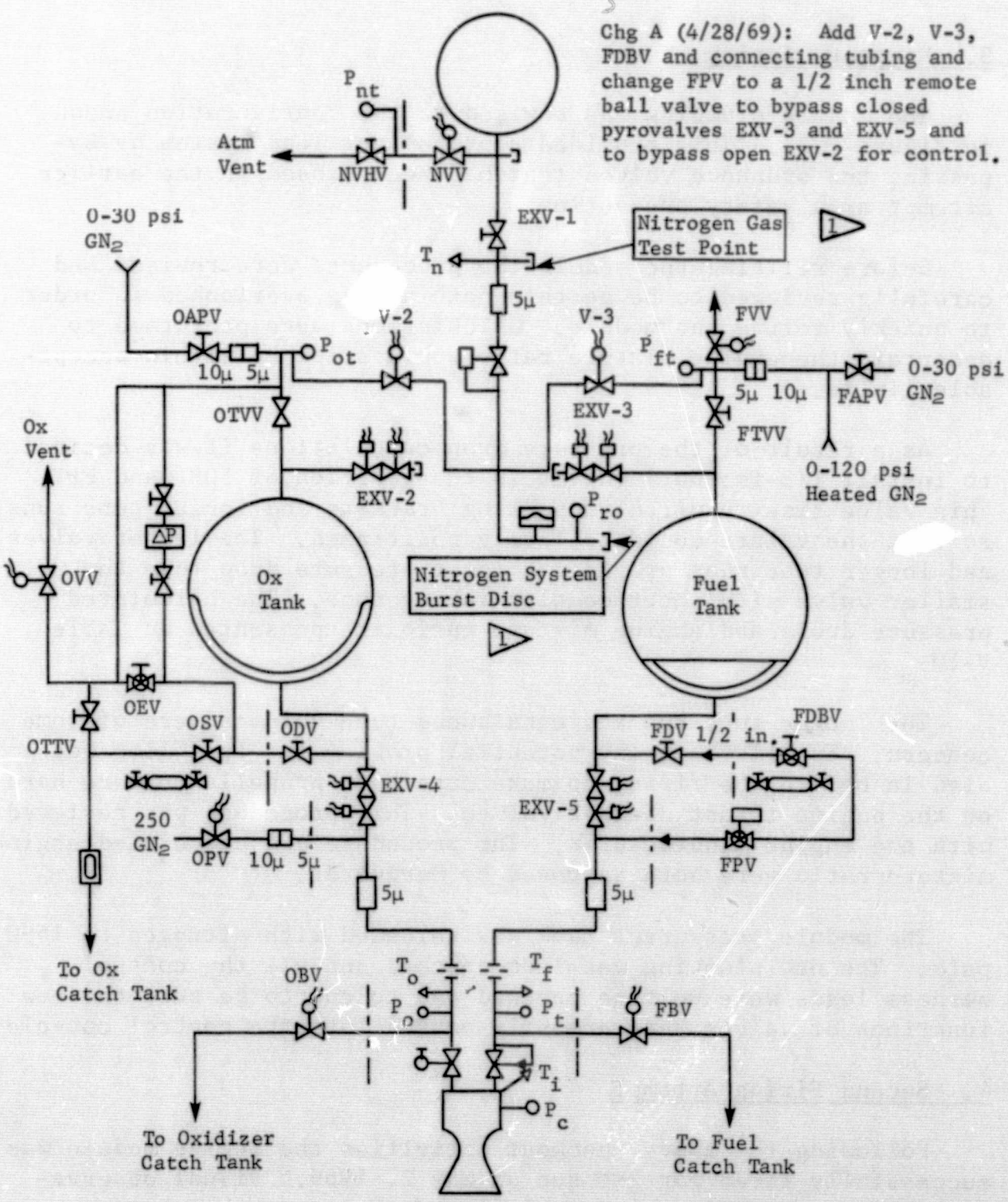

Fig. V-31 Firing Test Schematic (Change A)

Table V-10 Calculated Propulsion Module Performance (Revised Fuel Feed System)

A. Calculated Pressure Drop - Revised Fuel System

1/4 in. tubing - fuel tank to FDV valve:	7.1 psi
FDV valve - (corroborated in H_2O flow test):	7.8 psi
1/4-in. tubing - FDV to 1/4 x 3/8 union:	0.4 psi
1/2-in. tubing and two 1/2-in. ball valves:	0.2 psi
Assumed 1/2-in. fitting losses:	0.2 psi
3/8-in. tubing - module panel to filter tee:	0.4 psi
Total loss:	16.1 psi
Pressure drop - standard fuel system (actual):	40.0 psi
Less ordnance valve contribution (calculated):	1.6 psi
Pressure drop of remaining part of standard system:	38.4 psi
Pressure drop - entire feed system:	
Added tubing and valves:	16.1 psi
Unchanged part of system:	38.4 psi
Total System:	54.5 psi

B. Calculated Changes in Mass Flow and Mixture Ratio

Previous injector pressure drop:

P_f = 213 psig
P_c = 93 psig
ΔP_{inj} = 120 psi

Injector ΔP - revised system:

Previous P_f:	213 psig
Additional ΔP (54.5-40.0)	14.5 psi (use 15 psi)
Revised system P_f	198 psig
P_c (assumed unchanged)	93 psig
New ΔP_{inj}	105 psi

Injector flow rate change:

Previous fuel flow rate (actual) 0.146 lb_m sec.

New fuel flow rate: $0.146\ lb_m\ sec \left[\frac{105\ psi}{210\ psi}\right]^{1/2} = 0.137\ lb_m\ sec.$

Mixture ratio change:

Previous oxidizer flow rate (assumed unchanged): 0.226 lb_m sec.

$$\text{New mixture ratio} = \frac{0.226\ lb_m\ sec}{0.137\ lb_m\ sec} = 1.65$$

Previous mixture ratio (actual) = 1.54
Design mixture ratio = 1.59
From above:

Previous MR was $\frac{1.54}{1.59} \times 100 = 97\%$ of design MR

New MR will be $\frac{1.65}{1.59} \times 100 = 104\%$ of design MR

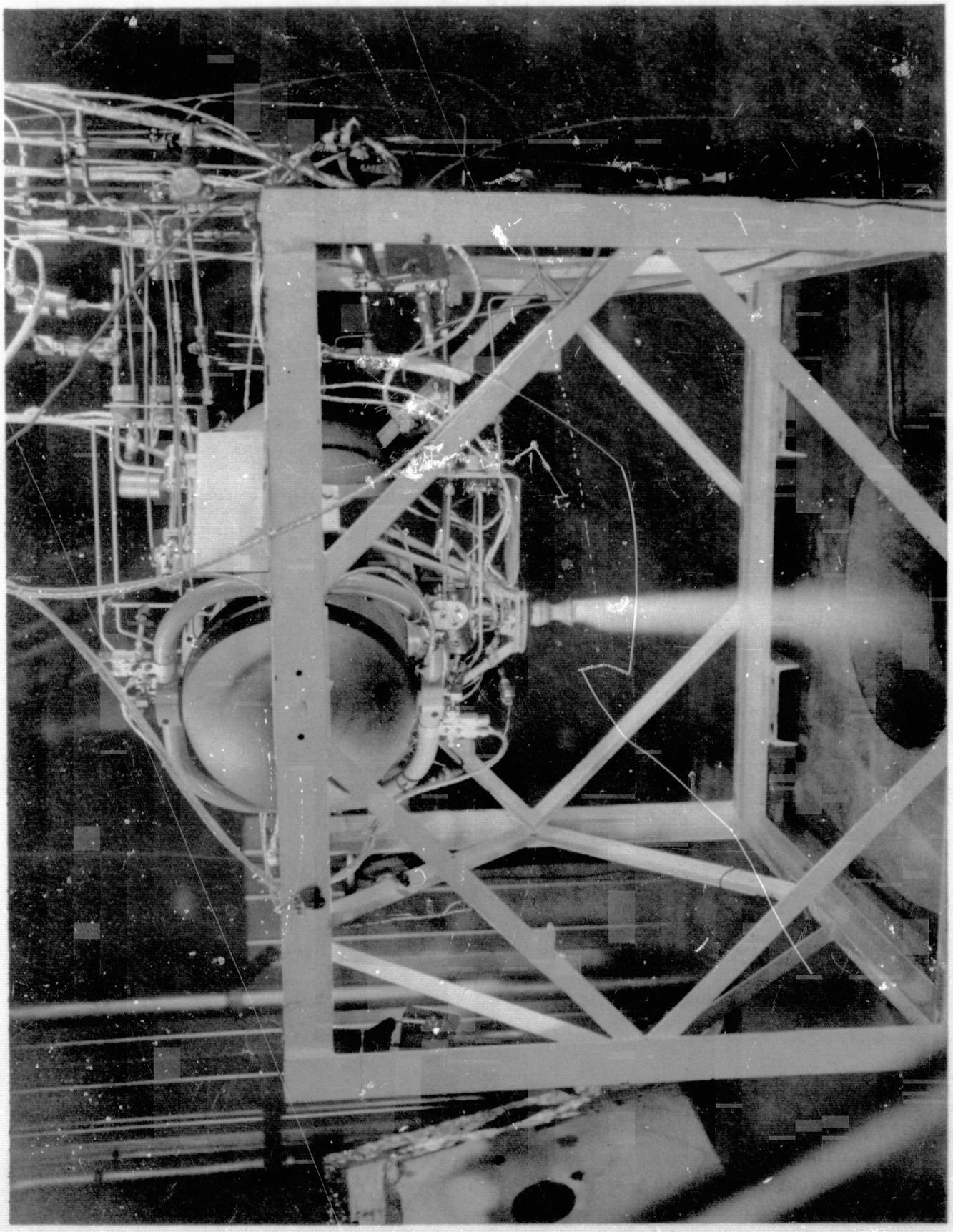

Fig. V-32 Module Firing Operation

G. SYSTEM PERFORMANCE

The firing performance of the engine is presented in Table V-11. From the table and the engine calibration data the following thrust and specific impulse were obtained.

	F	MR	I_{sp}
6000 ft	69.0	1.60	188
Vacuum Condition	108		294

This compares with the data from the initial firing on January 16, 1968.

	F	MR	I_{sp}
6000 ft	69.7	1.53	188
Vacuum Condition	109		294

From these data it can be seen that the performance parameters varied less than 1.0%, which is due to the change in mixture ratio resulting from the alteration of the module propellant feedline.

During the initial firing in 1968 there was no discernible pressure drop from the regulator outlet to the propellant tank top. The most recent firing showed a pressure drop of 3 and 4 psi to the oxidizer and fuel tank top respectively, resulting from the solenoid actuated valves. The regulator performance in the run condition, as opposed to the checkout condition, deserves explanation. In both the original and follow-on firing, an apparent shift in regulation pressure was noted as seen below:

	Original Firing	Follow-on Firing
Checkout pressure (psia)	260	255
Run Pressure (psia)	265	265

Investigation of the recording equipment reveals that consistent equipment was used for the appropriate checkout and firing. Also all calibration procedures were adhered to. The proper explanation appears to be that the lower reading during checkout results from the full regulator flow passing the pressure pickup outside of the module interface. Contrary to this, during the firing the pressure pickup is reading the pressure in a static tube that is sensing the complex flow split occurring in the distribution cross. Hence the checkout configuration is sensing the effect of a velocity head in a smaller tube, the pressure drop through the tube from the tubing cross to the pickup, and the loss associated with the 90 deg turn through the cross.

Table V-11 Propulsion Module Performance

Parameter	Predicted Value	T + 0 sec	T + 5 sec*	T + 140 sec	T + 275 sec	T + 280 sec
Burn Time (sec)	280	---	---	---	---	280
GN Tank Pressure, P_{nt} (psia)	1550	1590/1040	1035	770	535	530
Pressure, Regulator Outlet, P_{ro} (psia)	255	265	265	265	265	265
Pressure, Oxidizer Tank, P_{ot} (psia)	255	272	262	263	262	262
Pressure, Fuel Tank, P_{ft} (psia)	255	272	261	262	261	261
Pressure, Oxidizer Feedline, P_o (psia)	212	272	213	213	212	213
Pressure, Fuel Feedline, P_f (psia)	210	275	215	215	215	215
Chamber Pressure, P_c (psia)	105	0	104	104	104	104
Flow Rate, Oxidizer, w_o lb_m sec	0.226	0	0.226	0.226	0.226	0.226
Flow Rate, Fuel, w_f lb_m sec	0.137	0	0.141	0.141	0.141	0.141
Mixture Ratio, MR (oxid/fuel)	1.65	----	1.60	1.60	1.60	1.60

*Values read at stabilized conditions between T + 5 sec and T + 30 sec.
TVC Response: Opening oxidizer = 0.0119 sec, fuel = 0.0089 sec;
Closing oxidizer = 0.0087 sec, fuel = 0.0089 sec.

Ignition 0.0008 sec after oxidizer TVC full open.

H. PARTS INSPECTION

The cause of the system abort was discussed thoroughly in Section F of this chapter and will not be discussed further here. Several other parts were examined after the firing to determine what if any degradation had taken place.

1. Oxidizer Tank

The diaphragm of the oxidizer tank was recycled back to its original position and leak checked. The leakage determination was made with gaseous nitrogen at 1.0 psi differential pressure. The leakage value was 9.6 std cc/hr. This value compares to 0.16 std cc/hr determined at acceptance testing of the unit, and 78 std cc/hr for the component tank delivery that had not been resterilized. The tank has not been disturbed pending delivery of the parts to JPL.

2. Regulator

The regulator was disassembled following the firing to determine the cause of the sticking experienced before sterilization. Figures V-33 show the condition of the spring guide and cap assembly as they were disassembled. The photos show an accumulation of a dark film residue located between the surfaces of these parts. When these parts were removed there was some adhesion of the parts. A light oil was found on the back side of the diaphragm that caused the discoloration on the spring guide.

The inlet and outlet sections of the regulator showed no accumulation of any foreign material. The integral inlet filter was also in a good clean condition.

The regulator surfaces shown in the photos were not corroded in any way. The film that caused the sticking was dark in color resembling molybdenum disulphide and was easily wiped off. The spring pressure forces that were undisturbed for 15 months contributed to the parts adhesion.

The regulator manufacturer, Sterer Engineering, has confirmed that a light oil was placed behind the diaphragm to aid in positioning it during assembly. The project engineer for this regulator reproduced the sticking by placing oil between the spring guide and cap assembly on a unit at the Sterer plant.

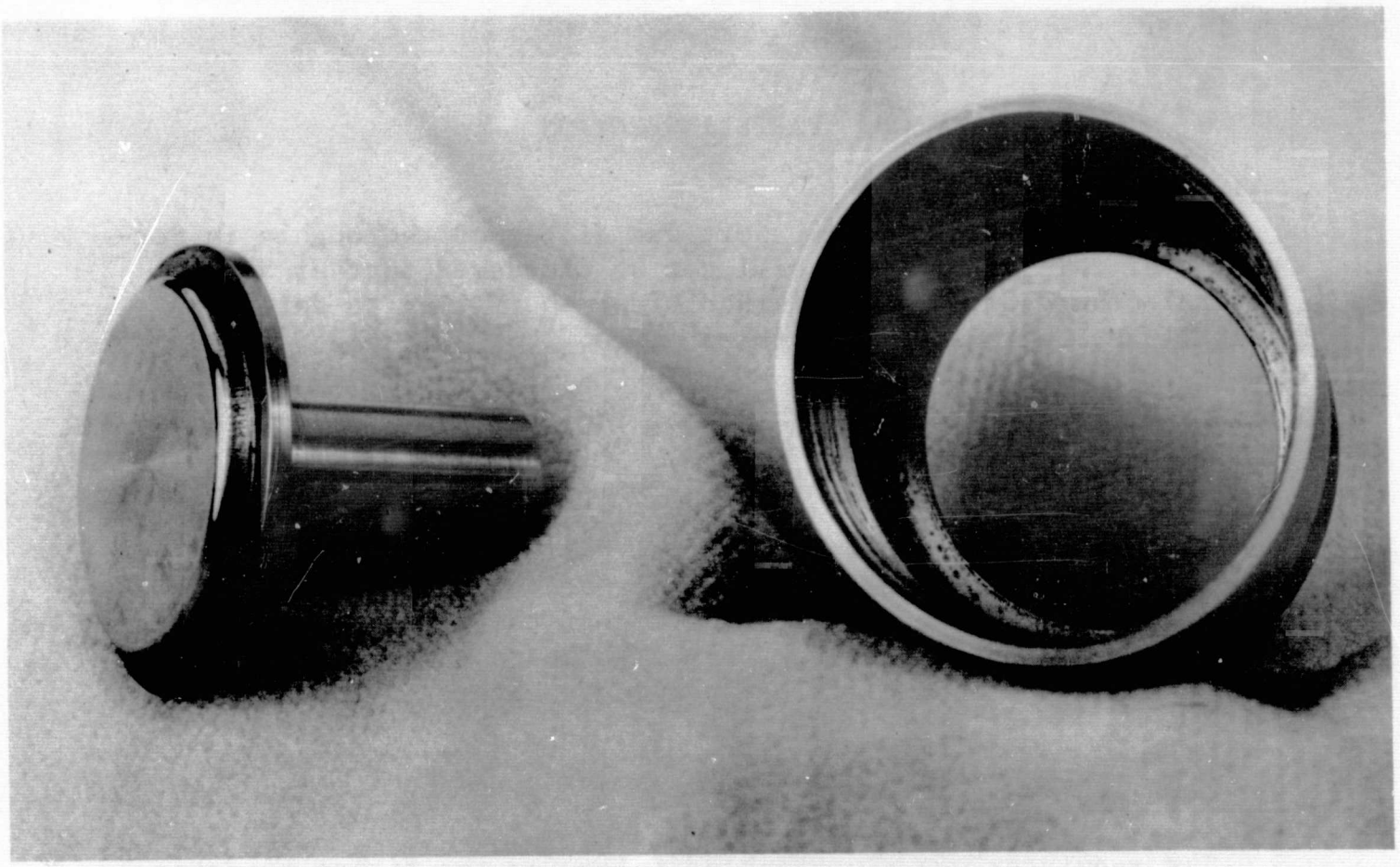

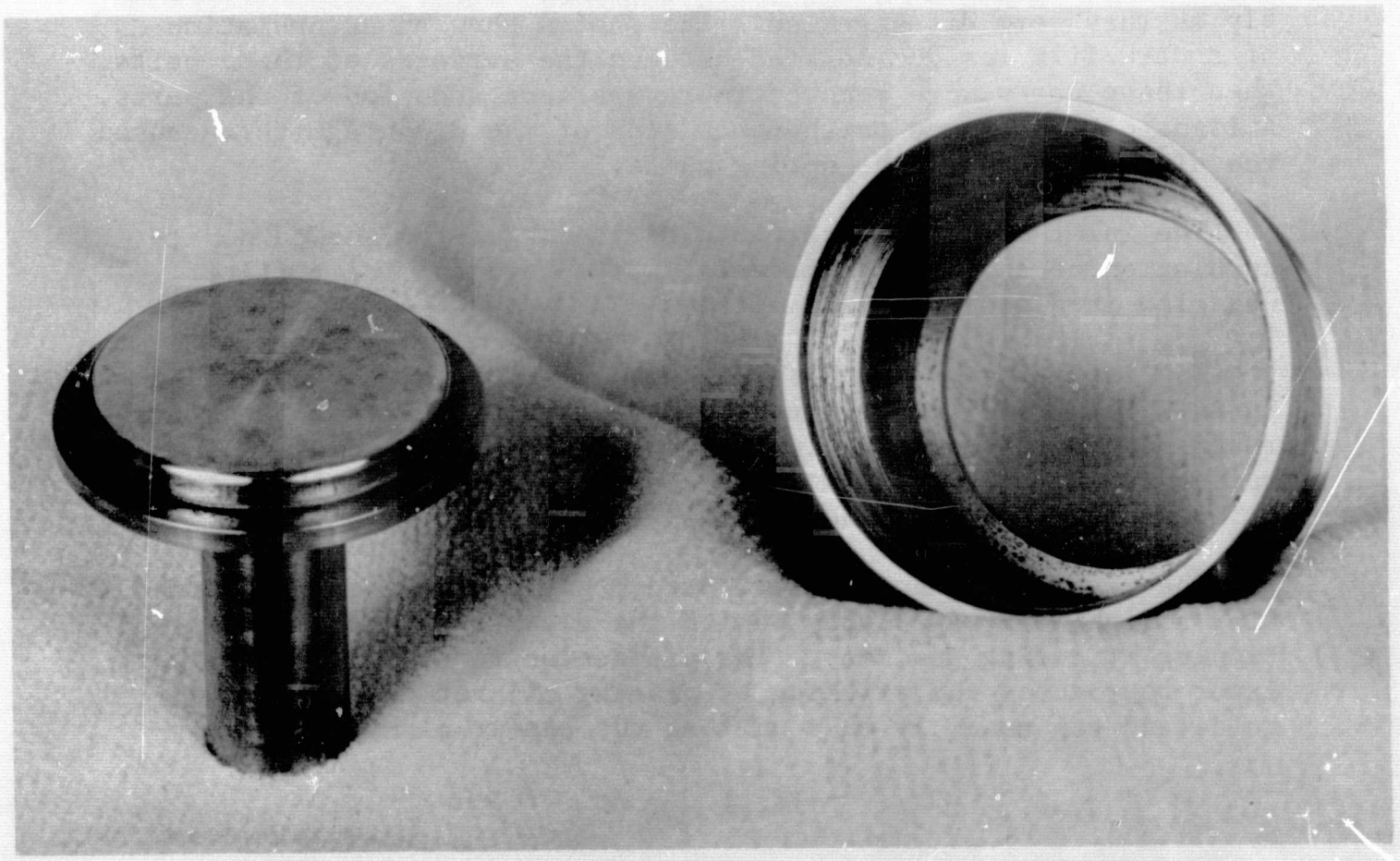

Fig. V-33 Regulator Spring Guide and Cap Assembly

The suggested corrective action is either to knurl these surfaces or machine lands in the cap assembly to reduce the finely machined contact area.

3. Hand Valve

The hand valve located in the fuel drain system was removed and disassembled to determine the cause of valve leakage. Figure V-34 shows the condition of the valve stem. The uneven loading or seating impression on the stem can be seen in the figure. Further there is evidence of scarfing on the side of the stem. This evidence is indicative of overloading the valve stem due to excessive torque applied to the valve.

The design is based on a steel valve, but for this program it was modified to use aluminum. As a result the recommended torque was 10 in.-lb with a maximum of 20 in.-lb. Experience with the valve led to the finding that leakage could be expected at 10 in.-lb and instructions were issued to raise the torque to 17 in.-lb with the maximum of 20 in.-lb. This problem would be expected, operating so close to the design limit.

Figure V-35 shows the condition of the Teflon chevron seals and general contamination in the stem area. The condition of cold flowing of the Teflon seals is a duplicate of the valves tested in the component task. This valve was not disassembled following th the initial scope of work.

Leakage data for this valve shows leakage was zero at the time of refurbishment and it was therefore installed in the liquid drain line. Leakage was evident following propellant loading activities. It was overstressed at that time.

4. Solenoid Valve

The solenoid valve changes resulting from a breakdown in the coil insulation were presented on page V-45. The valve leakage and coil dielectric strength history is presented in Table V-9. As can be seen the dielectric current leakage increased from 104 μamp to 114 μamp during this series of tests. This change compares to an increase of 272 μamp with the original design. No operational problems with the valve were encountered during the second test series.

5. Flange Joint

The coating of the soft aluminum washer and the improved installation procedure used in the ordnance valve seal as described on page V-48 was completely successful.

6. Lines and Joints

Several line and joint configurations were used in the module design to accumulate as much data as possible. Lines of 301 stainless steel, of 6061-T6 aluminum and several transition joints from titanium to steel and from steel to aluminum were used. Both AN and welded connections in addition to the serrated washer connection at the ordnance valve were used. All joints and lines performed satisfactorily. There were no leaks in the system. The line rupture experienced as a result of the improper ordnance valve assembly was not attributable to the tube design.

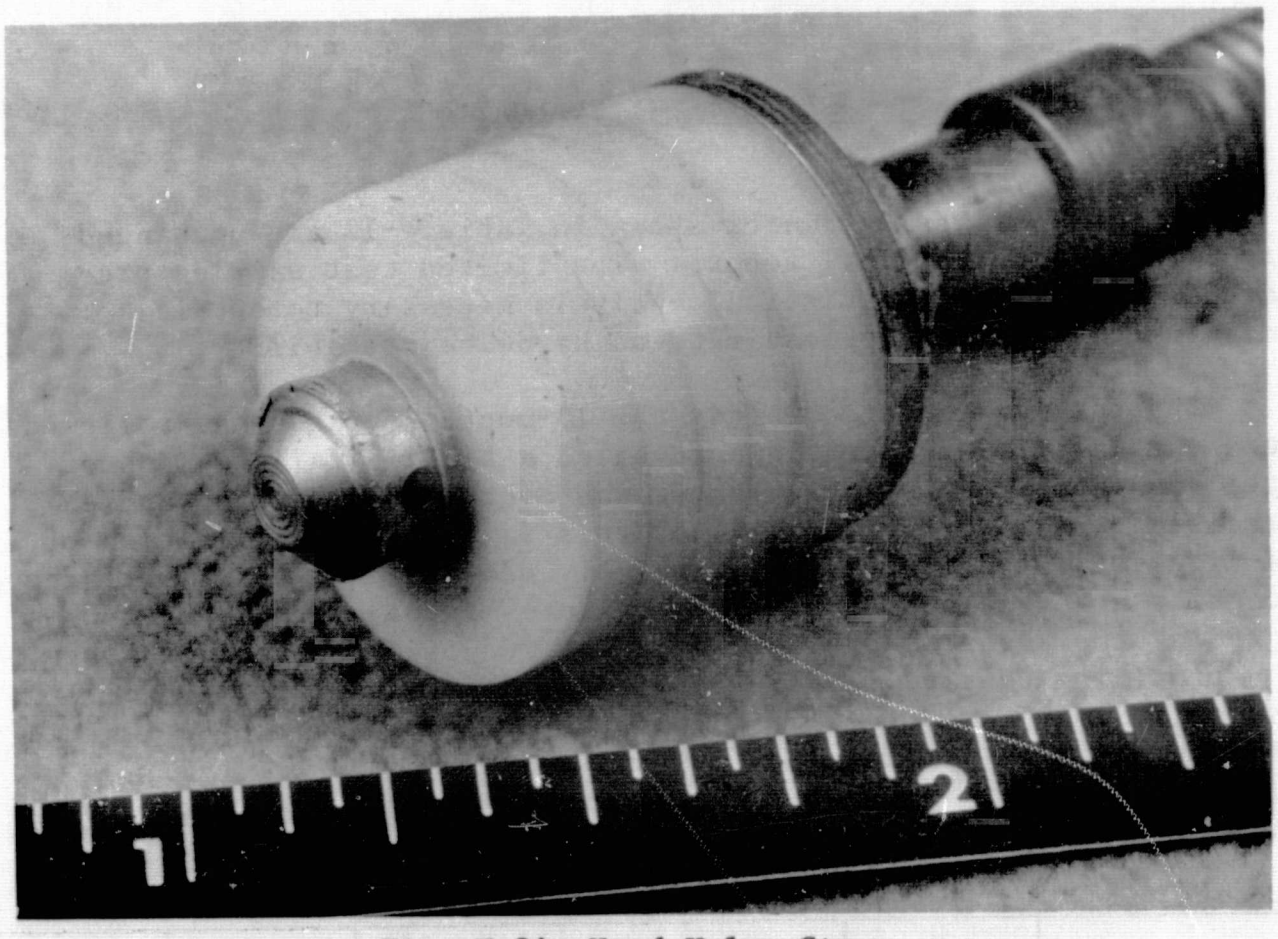

Fig. V-34 Hand Valve Stem

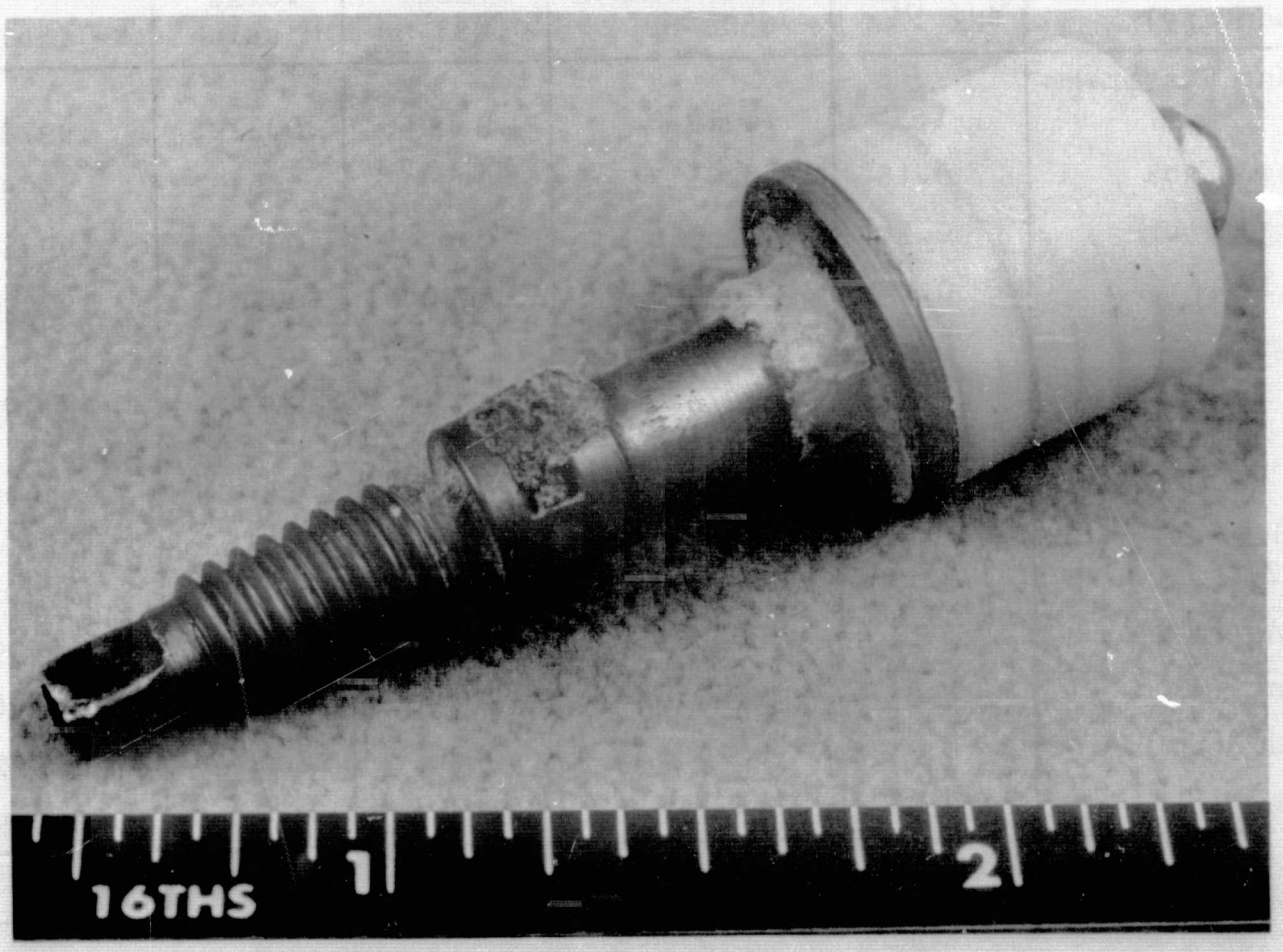

Fig. V-35 Hand Valve Stem Seal

I. RELIABILITY EVALUATION

The reliability estimates shown in Table V-12 are unchanged from Part I of the final report. The limited test samples preclude an extensive statistical analysis necessary to obtain a meaningful quantitative estimate of hardware reliability.

The testing conducted after the 15-month storage that followed the initial firing operations revealed a binding failure mode of the regulator. This failure mode was overcome by tapping and exercising regulator. The cause of this failure was a migration of a light oil used in the valve assembly between two faying surfaces, causing a severe adhesion. This failure may be overcome by downgrading the surfaces by knurling or by reducing the contact area by providing contact lands. In either case the filure is understood and may be corrected; therefore, no reduction of the generic failure rate is justified.

Table V-12 Sterilizable Liquid Propulsion System Reliability Estimate

Components (Quantity)	G_{FR} 10^6	Launch and Cruise Phase, 6500 hr	Burn Phase, 0.083 hr	Total Mission	Reliability
Propellant Diaphragm Tank (2)	1.5	.001950	.000246	.002196	.997804
N_2 Storage Tank	0.18	.000117	.000015	.000132	.999868
Press Regulator	0.7	.000046	.000058	.000105	.999895
Filter (3)	0.04	.000008	.000009	.000017	.999983
Ordnance Valve N.C. (5)	1000	--	--	.0050	.995000
Ordnance Valve N.O. (5)	10	--	--	.000050	.999950
Thrust Chamber Valves (2)	2.27	.000295	.000374	.000669	.999331
Orifice Assembly (2)	0.01	.000001	.000002	.000003	.999997
Test Point (7)	0.01	.000046	.000006	.000052	.999948
Lines and Fittings	0.1	.000065	.000008	.000073	.999927
Structure	0.001	--	--	--	.999999
Total System					.991581